Chem Soc Rev

From Fundamentals to Applications: A Toolbox for Robust and Multifunctional MOF Materials

Journal:	*Chemical Society Reviews*
Manuscript ID	CS-REV-08-2018-000688
Article Type:	Review Article
Date Submitted by the Author:	22-Aug-2018
Complete List of Authors:	Kirchon, Angelo; Texas A&M University, Chemistry Feng, Liang; Texas A&M University College Station, Chemistry Drake, Hannah; Texas A&M University College Station, Chemistry Joseph, Elizabeth; Texas A&M University, Chemistry Zhou, Hong-Cai; Texas A&M University, Chemistry

Journal Name

ARTICLE

From Fundamentals to Applications: A Toolbox for Robust and Multifunctional MOF Materials

Received 00th January 20xx,
Accepted 00th January 20xx

DOI: 10.1039/x0xx00000x

www.rsc.org/

Angelo Kirchon†[a], Liang Feng†[a], Hannah F. Drake†[a], Elizabeth A. Joseph[a], and Hong-Cai Zhou*[a, b]

In recent years, metal–organic frameworks (MOFs) have been regarded as one of the most important classes of materials. The combination of various metal clusters and ligands, arranged in a vast array of geometries has led to an ever-expanding MOF family. Each year, new and novel MOF structures are discovered. The structural diversity present in MOFs has significantly expanded the application of these new materials. MOFs show great potential for a variety of applications, including but not limited to: gas storage and separation, catalysis, biomedicine delivery, and chemical sensing. This review intends to offer a short summary of some of the most important topics and recent development in MOFs. The scope of this review shall cover the fundamental aspects concerning the design and synthesis of MOFs and range to the practical applications regarding their stability and derivative structures. Emerging trends of MOF development will also be discussed. These trends shall include multicomponent MOFs, defect development in MOFs, and MOF composites. The ever important structure-property-application relationship for MOFs will also be investigated. Overall, this review provides insight into both existing structures and emerging aspects of MOFs.

Introduction

In the mid-1990's a new class of porous materials was discovered, resulting in a long-lasting impact on the field of chemistry, biology, physics, and material science. These materials are known as Metal-Organic Frameworks (MOFs) or Porous Coordination Polymers (PCPs).[1] Due to their wide range of structures and functionalities MOFs have been widely accepted for applications which include gas storage and separation, catalysis, biomedical delivery, chemical sensing, as well as other applications not mentioned here.[2-19] In order to fully understand the scope of this review and MOFs in general, there are three key concepts that must first be introduced. These concepts are: molecular metal-organic hybrids, frameworks, and porosity.[1, 3, 20, 21]

When first approaching molecular metal-organic hybrids, it should be noted that various components contribute to the final structural design of the framework; linker design, linker chelation, binding affinity, number of open metal sites on the clusters, strength of the metal-organic bond, and the symmetry of the moiety. Together, all of these complex factors play a significant role in the final structural design, functionality and application of a MOF.

Furthermore, MOFs extend beyond the formation of just one metal to linker coordination bond through a second metal unit (M-L-M) in a geometrical fashion generating one-, two-, or three-dimensions creating a multi-dimensional frameworks. The framework itself can extend infinitely in any direction according to the linking design of the initial metal cluster formation. This initial framework will extend to make a polymer type structure, complete with voids and channels, a porous, sponge like material. The porosity of a MOF is defined as the ability to maintain a porous structure without guest molecules in the pores. This means that when all guest molecules are removed under vacuum, the pores do not collapse, resulting in permanent porosity.

Keeping these concepts in mind, this review aims to the lay out the recent developments that have allowed scientists to design and synthesize multi-functional MOF platforms for various applications.

Design and Synthesis of MOFs

[a] Department of Chemistry, Texas A&M University, College Station, Texas 77843-3255.
[b] Department of Material Science and Engineering, Texas A&M University, College Station, Texas 77843-3003, United States.
† These authors contributed equally to this work.

The synthesis of a MOF is traditionally accomplished by hydrothermal or solvothermal techniques in which crystals are slowly grown from a high-temperature solution.[22] Organic ligands remain intact throughout the synthetic process, meaning that their unique functionality can be preserved within the framework. Synthesis of mixed-linker MOFs is also possible, with more than one type of organic ligand used in the synthetic process, resulting in multiple functionalities within a single structure. For MOFs, a templating approach is designed with the final application of the MOF in mind. For example, MOFs intended for gas storage use a coordinating solvent such as N, N-dimethylformamide or water in the synthesis. These solvents have the ability to bind to an open metal site so that when the solvent is evacuated during activation, the open metal sites are exposed, allowing for interaction with the target gas molecules.[23, 24] In MOFs, ligands are reversibly bound and the resulting slow growth of the MOF crystals allows for defects to be corrected during the synthetic process due to the inherent lability of the bonds. This feature means that the resulting MOF crystal will be near equilibrium defect density.[23] This results in regularity in the structure with respect to the presence of the defects.

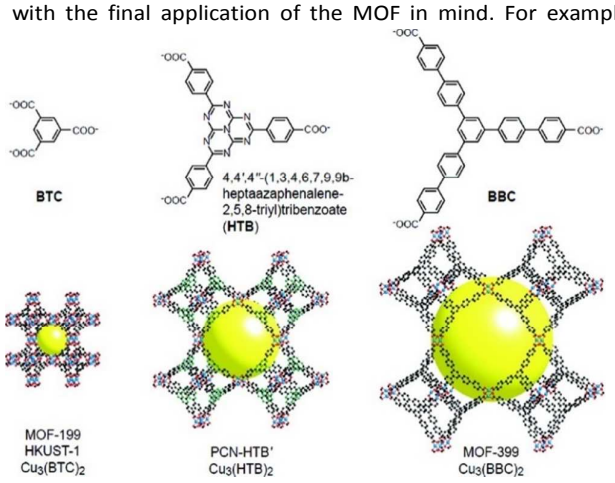

Fig. 1 Structures of organic linkers (top). Single crystal structures of MOF-199, PCN-HTB', and MOF-399 (bottom). The yellow sphere in the structure indicates the open space in the pore. Cu, blue; C, black; O, red; and N, green. The hydrogen atoms are omitted for clarity. Reprinted with permission from Reference 8. Copyright © 2011 American Chemical Society.

Isoreticular Expansion

Isoreticular expansion, also referred to as scale chemistry or isoreticular synthesis, is the expansion of the same topology of a structure utilizing increasing length of similar ligands to make ultra-large-pore MOFs. This strategy is often used for the enlargement of pore sizes, increasing the surface area, and tuning of the pore surface functionalization.[8, 20] Isoreticular chemistry is achieved through the use of building units of increasing size while maintaining the same coordinate geometry as the parent MOF. This strategy produces solids with the same framework topology but larger dimensions and increased pore and window sizes.[5] In an isoreticular series, a parent MOF maintains the original literature name for the MOF. However, subsequent MOFs in an isoreticular series are often named IRMOF to denote that they were designed using isoreticular expansion of the original parent structure. With older MOF series, this naming system does not always apply. This is because MOF nomenclature is still widely varied in the scientific community.

Another consideration when preparing an isoreticular series is that the reaction conditions must result in the same inorganic cluster obtained in each reaction.[8] This is necessary to ensure that coordination geometry and topology present in the parent MOF is maintained. A changing size, shape, coordination environment, or number of open sites at a metal cluster often results in a change in the framework topology. Although maintaining as many of the parent MOF characteristics is typical of isoreticular expansion, there have been examples of isoreticular expansion using different metal clusters of the same topology. A rather famous example was demonstrated in HKUST-1 where isoreticular expansion was demonstrated with three separate metals, Zn^{2+}, Fe^{2+}, and Cr^{2+} in addition to the original Cu^{2+}.[8, 25-29]

Prior to the discovery of isoreticular synthesis, the most common approach for MOF building involved reticular synthesis. Reticular synthesis refers to a synthetic method where the starting materials do not maintain their structure during the reaction in the formation of an extended structure. This leads to comparatively poor coordination between products and reactants. In contrast to reticular synthesis, isoreticular synthesis achieves an extended network by starting with a well-defined and rigid molecular building block that is intended to maintain its structural integrity during the synthesis process.[6]

Isoreticular synthesis is predominantly characterized by the increase in the pore size by increasing the linker size. However, there are limits to the size and stability of a MOF structure grown in this manner. As the linker size increases, the structure becomes more prone to collapse when the guest solvents are removed, as size is often inversely proportional to stability in these structures. A famous example of this was with the Langmuir surface areas of UiO-66 and UiO-67. Their surface areas are 1187 and 3000 m^2g^{-1} respectively, but UiO-67 is significantly less stable than UiO-66.[9, 30] Thus, the long-term objective of isoreticular synthesis is to build structures that will be robust with increasing size.[6, 7, 9, 10] Other famous MOF series parent structures used for isoreticular expansion are MIL-53, MIL-88, and MIL-47.[31-34]

One of the first examples of an isoreticular MOFs series was based on MOF-5 ($Zn_4O(R_{1,10,12,16}\text{-BDC})_3$, R_1=H, R_{10}= BPDC, R_{12}= HPDC, R_{16}= TPDC) with variations on the MOF-5 BDC linkers. In this particular study, the pore functionality and size were varied without changing the cubic topology between MOF variations.[7] The diameter of the pores for the MOF-5 series was reported as 12.6 Å, 18.5 Å, 21.4 Å, and 28.8Å with increasing sizes of the linker variations, R= H, BPDC, HPDC, and TPDC respectively. Another successful example of using the isoreticular expansion strategy was in the synthesis of a series

of Zr-MOFs, $Zr_6(\mu_3\text{-}OH)_4(L_{1\text{-}4})_3$(NU-1101-1104, L_1=$PyXP^{4-}$, L_2=$Por\text{-}PP^{4-}$, L_3=$Py\text{-}PTP^{4-}$, and L_4= $PorPTP^{4-}$) by Wang and coworkers.[35] In their study, the geometric surface areas of NU-1101 to NU-1104 were calculated using a rolling probe method that was independent of Brunauer-Emmet-Teller (BET) theory, giving 4422 m^2g^{-1}, 4712 m^2g^{-1}, 5646 m^2g^{-1}, and 5290 m^2g^{-1}, respectively for NU-1101 to NU-1104.[36]

During the initial investigation into the IRMOF-5 series, it was noted that with increasing expansion of the linkers in the framework, there was an increased likelihood for interpenetration, which is also known as catenation. This is a common problem for isoreticular synthesis series of MOFs.[7, 10] When interpenetration is present, there is always a reduction of surface area, pore volume, and availability of active sites in the MOF. This is unfavorable for applications involving large molecules such as gas storage, gas separation, catalysis, and drug delivery, but can be favorable for applications involving small molecules such as hydrogen.[4-19] The probability of forming an interpenetrated network is closely related to the framework topology. As a result, significant research efforts have been directed at topology guided design to address the problems associated with isoreticular expansion.[37-40]

Topology-guided design

An alternative to isoreticular expansion is topology-guided design. This approach was originally designed to avoid interpenetration in MOFs by changing the synthetic conditions and increasing the steric hindrance of the ligands incorporated in the framework.[7, 41-44] In this strategy, the "template" to build a MOF is based on the non-interpenetrated topological structure and their synthetic conditions.[9] It is through this method that MOFs can be designed based on preconceived structures, resulting in desirable properties and high synthetic accessibility.[10] In topology-guided design, the configuration of the MOF is dependent upon the metal-containing building units, the organic ligands, and the symmetric complement of the original network.

A famous example of topology-guided design was by Gomez-Gualdron and coworkers in 2014, demonstrating **csp**, **scu**, and **ftw** topologies using square-shaped tetratopic ligands and Zr_6 clusters.[45] The organic linkers were selected based on two design criteria: (1) the linker should possess a planar geometry and (2) the linker should have four carboxylate groups in a rectangular shape close to that of a square.[46] This particular strategy resulted in a structure with the highest surface area with a low propensity for structural catenation in a Zr-MOF possessing a **ftw** topology. This particular **ftw** structure contained 12-connected $[Zr_6(\mu_3\text{-}O)_4(\mu_3\text{-}OH)_4]$ clusters and tetratopic linkers connected in a way that forces the linkers to connect across the face of the unit cell. The structure was crystallized in the Pm3m space group where the metal clusters occupy the vertices.[45]

In the use of a topology-guided design, the orientation of the ligand is as important as the connectivity and symmetry of the target MOF. A common strategy uses steric hindrances and the resulting energetically unfavorable orientation of ligands to force the synthesis to give a specific topology. This strategy is often referred to as controllable conformation. Liu and coworkers used this strategy to introduce triple-bond spacers between adjacent phenyl rings and carboxylate groups to exert conformational control in PCN-228, PCN-229, and PCN-230.[47]

To avoid interpenetration in a MOF system, an opportunistic technique is to use a topology that is impossible to translate in all directions without overlapping upon itself. An example of this was done with the **flu** topology, a high symmetry edge type translated network of fluorite (**flu**).[23, 48, 49] The Zr-MOF variant of this topology was based on the **flu** cubic close packing of Ca(II) in which the tetrahedral cavities were filled with F^- anions. In this structure, the octahedral cavities are left unoccupied. For the flu topology in Zr-MOFs, it is impossible to translate in all directions without overlap, avoiding interpenetration and creating high permanent porosity.[6, 50]

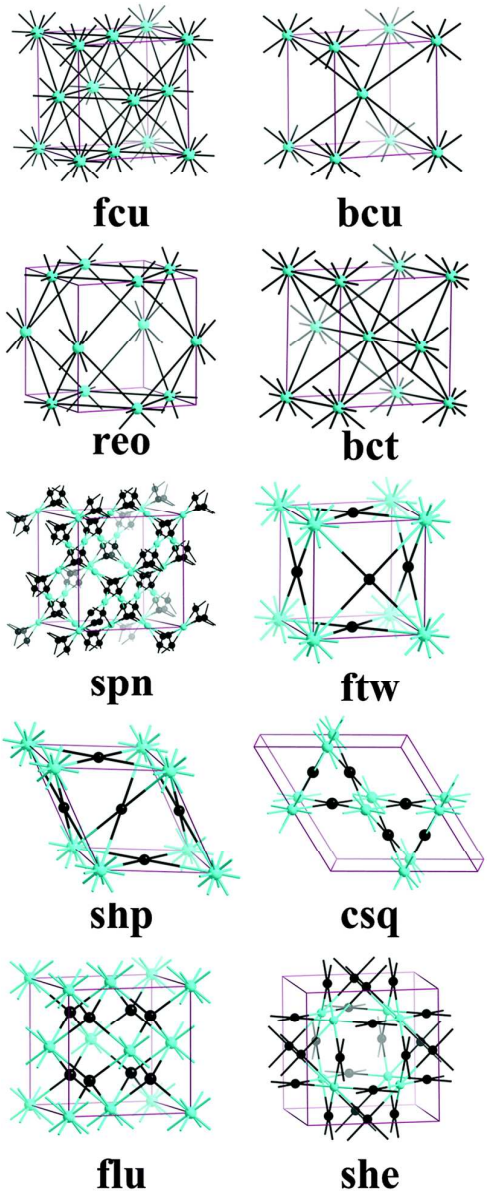

This particular strategy was first exhibited in a Zr-MOF by Friedrichs and coworkers in 2003.[6] Other examples of this type of strategy are PCN-521 ($Zr_6(\mu_3\text{-}OH)_8(OH)_8(MTBC)_2$) and PCN-700 ($Zr_6(\mu_3\text{-}O)_4(\mu_3\text{-}OH)_4(OH)_4(H_2O)_4(Me_2\text{-}BPDC)_4$).[51, 52]

Fig. 2 Representative network topologies in many reported MOFs. The topological symbols have been summarized in previous reviews. For example, **fcu** indicates a face-centered cubic net; **scu** and **ftw** refer to (4,8)- and (4,12)- connected network; **reo** originated from the packing of ReO_3 lattice. Reprinted with permission from reference 10. Copyright © 2016 Royal Society of Chemistry.

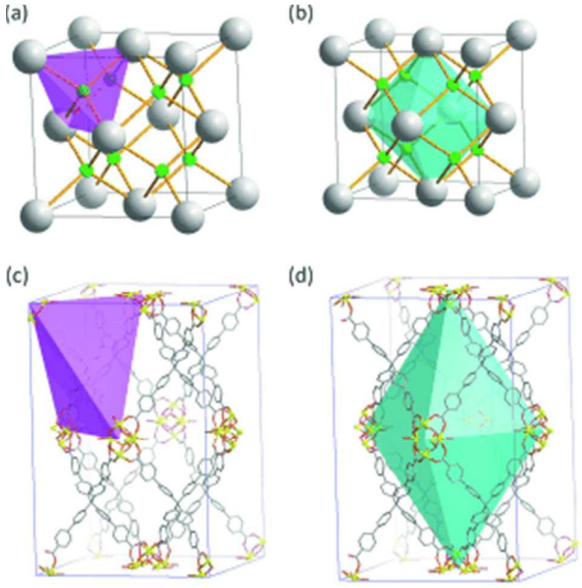

Fig. 3 a) A representation of the fluorite structure type where the fluoride anions fill the tetrahedral cavities (one is highlighted in purple). Gray Ca and green F. b) The unoccupied octahedral cavities (turquoise) in the fluorite structure. c) The augmentation of the tetrahedral node of fluorite structure that results in a MOF with the same topology but larger pores. C gray, O red, and Zr yellow. d) The representation of an octahedral cavity in PCN-521. Reprinted with permission from Reference 51. Copyright © 2013 Angewandte Chemie.

Modulated synthesis

Modulated synthesis refers to the use of modulating agents that regulate the coordination equilibrium of a growing MOF. Modulating agents are chemical species that coordinate to the metal clusters in a similar fashion but have a lower binding affinity than the desired ligand. The modulator binds reversibly to the metal cluster, slowing down the formation of the framework by inhibiting coordination sites and slowing the formation of nucleation sites.[53, 54] This slows the rate of formation of the framework, allowing for the equilibrium to correct and regulate the defects, resulting in the increased crystallinity in the product. Acids are one of the most commonly used modulators in MOF synthesis. Some examples of acids used as modulators include benzoic acid, hydrochloric acid, acetic acid, trifloroacetic acid, formic acid, and water.[53, 55-58] This controlled synthesis approach often leads to anisotropic growth of MOF crystals.[55] This coordination modulation method greatly improves the reproducibility of a synthetic procedure. This approach also allows for the features of the crystals, mainly size, morphology, and crystallinity, to be fine-tuned. Prior to the development of this synthetic method, MOF synthesis often resulted in small microcrystalline powder samples.[22]

It has been shown that there may be a variety factors that influence the synthetic pathway in the modulated synthesis approach. Strong acids can reduce the pH, thus suppressing deprotection of organic linkers. As coordination to a metal center or cluster is dependent upon deprotection of the organic linker, the rate of MOF formation is often inversely related to concentration of a strong acid as a modulating agent. It should be noted however that the addition of different kinds of acids and of different concentrations can lead to different metal clusters forming during synthesis producing an impure product.[59] Likewise, varying the solvent during synthesis with the same acids as modulators can result in differences in structure.[60]

It is proposed that an *in situ* formation of coordination complexes between the metal cation and the modulator is the reason why larger and larger crystals can be obtained with an increased amount of modulator. The structures that result from this interaction serve as intermediates in the construction of the final MOF as it can be formed through an exchange reaction between the modulators and the bridging ligands.[56] It serves to reason that an increasing concentration of modulators would inhibit the formation of nuclei and nuclei growth leading to the formation of larger crystals in the resulting MOF.[10] In line with this reasoning, introduction of an excessive equivalence of modulating agent results in a complete lack of framework formation. One of the major challenges faced with the introduction of modulating agents is finding the right balance required to achieve the desired product as modulating agents have different effects on different frameworks.

Introduction of other species as modulating agents has also been explored. Both trifluoroacetic acid(TFA) and hydrochloric acid(HCl) have been demonstrated as effective modulating agents for the synthesis of UiO-66.[58] Both modulators provide a source of protons, which slows the hydrolysis of $ZrCl_4$ and the formation of active carboxylate species.

An early example of the modulated synthesis strategies reported in literature was reported by Schaate and coworkers for a Zr-MOF in 2011. Their study used the UiO-66 (Zr-BDC-NH_2), UiO-67 (Zr-BPDC-NH_2), and UiO-68 (Zr-TPDC-NH_2) MOF set and modulators of benzoic acid, acetic acid, and water in the formation of the MOF crystals. In their study, it was found that an increasing concentration of benzoic acid modulator resulted in larger crystals of UiO-66. This ability to tune the crystal morphology and size by varying concentrations of modulators such as benzoic acid worked for all three Zr-MOFs. In their study, Schaate and coworkers also indicated the crucial nature of water as a rate of crystal growth inhibitor in the

successful synthesis of the MOFs. It was by this synthetic method that the first single-crystal structure of a Zr-MOF, UiO-68, was reported.[56]

In other notable studies such as that of Wissmann and coworkers, it was demonstrated that certain modulators, such as formic acid, accelerated the formation of MOF crystals. In their study of Zr-FUM ($Zr_6(\mu_3\text{-}O)_4(FUM)_6$), they suggested that a possible reason for this accelerated formation was that formic acid was a direct product of the decomposition of N,N'-dimethylformamide and water. They suggested this indicated that the presence of formic acid affected the reaction equilibrium and the ratio of water present in the reaction system, making the reaction proceed more rapidly.[57]

A particularly useful study for the exploration of defect engineering that can be done with modulated synthesis comes from a rather comprehensive study of the effects that this technique exhibits on porosity and composition for the MOF UiO-66. In the study by Lillerud and coworkers., they explore the effect of pKa, pH, and concentration of a modulator on UiO-66 for the purpose of defect engineering.[61]

Post-synthetic modification

Post-synthetic modification, also referred to as post-synthetic functionalization, describes the tailoring of a MOF after the MOF has already been synthesized. It is a secondary step to functionalization that creates a versatile tool that allows us to create a variation of the parent MOF with identical topology. This approach leads to diverse functionalities and uncompromised structural stability.[62-70] In many cases, this route is employed when the target MOF cannot be easily obtained using traditional direct synthesis methods.[71] There are many types of post-synthetic modification including but not limited to: covalent functionalization, integral covalent modification, surface functionalization, post-synthetic metalation, post-synthetic exchange, dative post-synthetic modification, post-synthetic deprotection, post-synthetic polymerization, and post-synthetic cluster modification. Clearly, there are a variety of ways a MOF can be modified post-synthetically, and each of these forms of modification has the capacity to alter the physical and chemical properties of the framework.[72] This brief overview, will touch on the four main classes of post-synthetic modification: covalent, metalation, dative, and deprotection.[65, 72, 73]

Covalent post-synthetic modification

The concept of post-synthetic modification was first proposed by Robson in 1990,[74] but it took nearly a decade for reports of this method to appear in the literature, with the first successful method being covalent post-synthetic modification.[75] As is the case for this and more recent covalent post-synthetic modifications, most ligands used in this strategy contain a chemical functionality that does not interfere with MOF formation, but can be used as the site for modification in subsequent post-synthetic modification reactions.[73, 75-77] In addition to the MOF reported by Kiang and coworkers,[75] there were other early examples of post-synthetic modification in MOFs.[76-79] However, it was not until 2007 when the Wang and Cohen groups coined the term "post-synthetic modification" to describe the reaction of IRMOF-3 with acetic anhydride.[80] A more recent example of covalent post-synthetic modification is that of the highly stable isoreticular MOF series: PCN-56, PCN-57, PCN-58, and PCN-59 by Jiang and coworkers that was published in 2012. In PCN-58 and PCN-59, ($Zr_3O_2(OH)_2$(TPDC-$(CH_2N_3)_2$) and ($Zr_3O_2(OH)_2$(TPDC-$(CH_2N_3)_4$) respectively, the azide group was able to undergo a click reaction with alkynes to post-synthetically form triazole groups. In their study, it was revealed that loading of azide groups can be accurately tuned by varying the ratio of ligands containing azide groups during synthesis, ultimately allowing for a variety of functional groups to be anchored to the pore walls while maintaining control in regard to loading, functionality, and density of the substrates.[81]

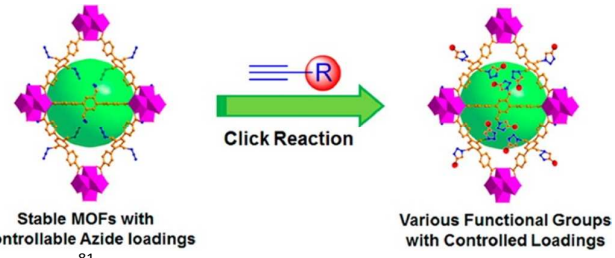

Fig. 4 Post-synthetic covalent modification using azide functional groups in PCN-58, which undergoes a click reaction. Reprinted with permission from reference 81. Copyright © 2012 Journal of the American Chemical Society.

Post-synthetic metalation modification

Another common post-synthetic modification technique is post-synthetic metalation and cluster modification, which are collectively referred to as coordination modification. In this type of modification, the coordination environment is altered by exchanging one metal for another or by modifying the metal cluster geometry.[65, 72, 73, 82] This is most often performed when only one metal is stable during the synthetic process, but the second metal, which may undergo side reactions during

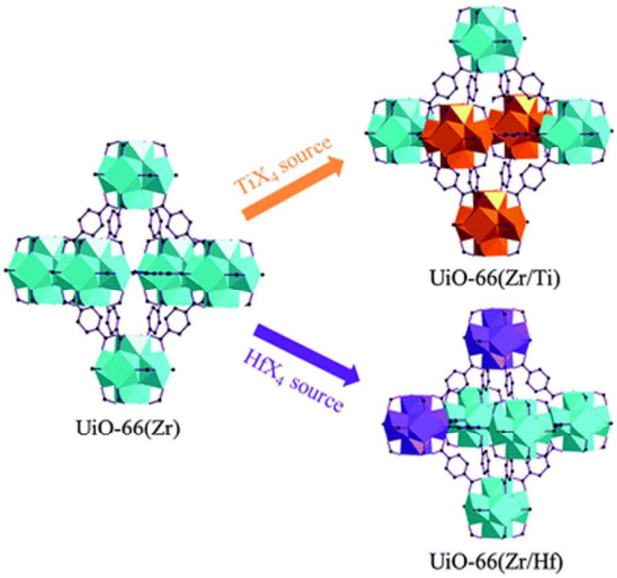

Fig. 5 Representation of Zr(IV) partial substitution in UiO-66 by Ti(IV) and Hf(IV) for the synthesis of UiO-66(Zr/Ti) and UiO-66(Zr/Hf). Reprinted with permission from Reference 10. Copyright © 2016 Royal Society of Chemistry.

synthesis, is postsynthetically incorporated into the framework. This provides novel functionality in the product, which is not obtainable using direct synthesis methods.[71] Post-synthetic metalation occurs almost quantitatively in a MOF. Perhaps one of the most widely studied post-synthetic metalation cases in MOFs is that of MOF-867, also known as UiO-67(bipy), which is composed of 2,2'-bipyridine-5,5'-dicarboxylate bridging ligands.[83] The structure of this MOF is similar to that of UiO-67, but it has additional accessible bipy sites lining the MOF pores. As Zr MOFs are highly stable, UiO-67(bipy) can undergo metalation in a single-crystal to single-crystal manner.[84] This particular MOF system can be subjected to post-synthetic metalation with a wide range of substrates such as CuCl, $CuCl_2$, $CoCl_2$, $FeBr_2$, and $Cr(CO)_6$.[84] In the UiO-67(bipy) system, the symmetry is altered from Fm3m to Pa3 as a direct result of the ordering of the metalated linkers.[71]

Furthermore, low valent metal ions and/or organometallic complexes have been incorporated into MOFs using various methods such as metallo-ligand installation, amine anchoring, phosphine anchoring, and more.[85, 86] This approach often aims to incorporate much of the functionality and applicability of organometallic pincer catalysts into MOF applications. For example, Lin and coworkers designed a strategy for post-synthetic installation of earth-abundant metal (M = Fe, Cu, and Co) for C–H amination and hydrogenation.[87] Amine anchoring was also reported by Li and coworkers.[88] for the installation of single Ru sites as chemo-selective catalysts for the hydrogenation of quinoline. Lastly, phosphine anchoring was recently reported by Humphrey and coworkers.[89] They detailed how uncoordinated phosphine sites in frameworks such as PCM-101 could be used to post-synthetically install soft metals such as Au, and Cu.

Post-synthetic deprotection

A recent emergence in the field of post-synthetic modification is post-synthetic deprotection. The concept of deprotection is that a protected functional group is introduced onto an organic linker, the linker is incorporated into a MOF under standard solvothermal conditions, then the protecting group is removed in a post-synthetic reaction to reveal the desired functionality. This type of post-synthetic modification is extremely useful for the prevention of interpenetration in MOFs.[72, 90] One of the earliest examples of this type of post-synthetic modification was published by Yamada and Kitagawa who referred to this type of modification as "protection-complexation-deprotection (PCD)". In their study, an *in situ* deprotection of an organic linker was observed, resulting in a functionalized MOF. The protection step involved acetylation of 2,5-diacetoxyterephthalic acid (H_2dacobdc). The complexation step involved combining H_2dacobdc with bipyridine and Zn(II) in DMF to obtain a MOF with a layered-pillar topology. In their work, the complexation step and deprotection step occurred in tandem. This approach resulted in free hydroxyl groups, resulting in intramolecular and intermolecular hydrogen bonding which is believed to stabilize the resulting MOF.[90]

MOFs can also undergo post-synthetic deprotection via thermolabile groups. This system was successfully demonstrated by the Telfer group and was proven to be most successful for open, non-interpenetrated MOFs.[91, 92] The approach of using thermolabile groups for deprotection has been demonstrated to enable the suppression of undesirable network interpenetration and support the post-synthetic expansion of cavities within the framework. .[93] The concept of thermolabile post-synthetic deprotection in MOFs was first demonstrated in 2010 by Telfer and coworkers using a Zn MOF with a thermolytically cleavable tert-butylcarbamate group on a biphenyldicarboxylate ligand. Their approach to deprotection was later expanded to produce a generally usable strategy for the single-crystal-to-single-crystal transformation of an organocatalytic MOF via heating .[94]

Dative post-synthetic modification

One of the most common approaches for tuning pore functionality in MOFs is through dative post-synthetic modification. Dative post-synthetic modification is a type of ligand modification that replaces one linker with another in the metal cluster.[64, 73] The use of dative modifications was first reported in HKUST-1 in 1999.[25] The main structure of HKUST-1 has a Cu(II) paddlewheel secondary building unit (SBU) in the MOF and is among the most widely studied examples of MOFs. In the report published in 1999, the authors noted that the coordinated axial water molecules of the secondary building unit could be removed by heating HKUST-1 at 100°C in air. The material could then be immersed in dry pyridine to obtain a material with pyridine molecules bound to the SBU. It is significant to note that this pyridine form of HKUST-1 could not be directly synthesized by solvothermal methods.[25, 73] Later studies with HKUST-1 demonstrated that modification of a desired substrate by vapors can also result in a dative type modification. This method is effective for the introduction of chemical tags for gas capture.[95, 96] Dative post-synthetic modification has many subclasses, one of exemplary significance is post-synthetic exchange (PSE).

Post-synthetic exchange

Post-synthetic exchange (PSE) is a special type of dative post-synthetic modification and is often referred to as bridging-linker replacement[97] or solvent assisted linker exchange (SALE).[98] As this particular MOF synthesis technique is relatively new, much work remains to be done to elucidate the driving forces that govern PSE transformations. The structural aspects and conditions for successful PSE are also not fully understood at this time.[99-104] As a result, most studies on PSE have examined a very specific category of MOFs, pillared-paddlewheel systems. This system features 2D sheets comprised of polycarboxylate paddlewheel structural building units connecting binuclear metal clusters. These metal clusters are pillared by ditopic nitrogen donor linkers. The strength of

the metal-oxygen bonds between the carboxylate moieties and the metal clusters in the 2D sheets exceeds the strength of the metal-nitrogen bonds between the clusters and the pillars allowing for easy exchange of the nitrogen containing pillars, but not the carboxylate sheets.[105] In a typical SALE procedure, a parent MOF will be immersed in a concentrated solution of linkers to undergo a heterogeneous reaction. A successful SALE results in a daughter material that features the linkers from the solution incorporated into a framework possessing the topology of the parent crystal.

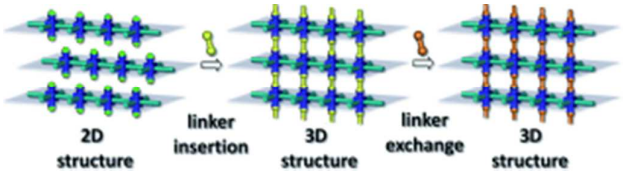

Fig. 6 Representation of Solvent Assisted Linker Exchange (SALE). Reprinted with permission from reference 97. Copyright © 2014 Angewandte Chemie.

There are a number of reported novel applications for the SALE technique. For example, this technique can be used to control the porosity of a MOF by inhibiting or introducing catenation into a MOF design.[106, 107] In a report by Mulfort and coworkers, the structure of Zn_2(tcpb)(dped)(DO-MOF) could be transformed into a non-catenated framework by use of the SALE technique. It is important to note, that if synthesized via the standard solvothermal technique, this MOF, an isostructural pillared-paddlewheel MOF, would form a two-fold catenated structure.[107]

In addition to catenation incorporation and inhibition, SALE can be used to generate larger cages and channels by replacing existing MOF linkers with longer linkers.[104, 108, 109] This approach is similar to the strategy used for isoreticular expansion in that a parent MOF template is used to design larger and larger MOFs, thus increasing pore volume, pore size, and surface area. Unlike isoreticular expansion, SALE can use the parent MOF to not only design, but also synthesize the daughter MOF directly. The first demonstration of using SALE in this way was achieved by Li and coworkers in 2013.[108] The MOF under study was bio-MOF-101 ($Zn_8(ad)_4(ndc)_6(OH)_2$) which is a MOF possessing **lcs** topology. SALE was employed to replace ndc with bpdc (2 Å larger than ndc) and then abdc (4Å larger than ndc) yielding bio-MOF-100 ($Zn_8(ad)_4(bpdc)_6(OH)_2$ and bio-MOF-102 ($Zn_8(ad)_4(abdc)_6(OH)_2$)

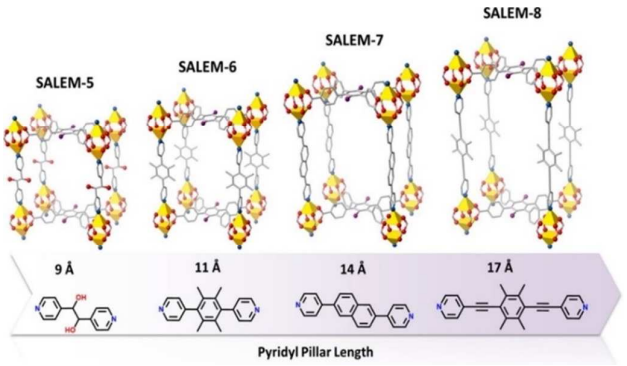

respectively. Both subsequent MOFs synthesized by SALE had

Fig. 7 Increasing pore size in an isoreticular series of paddlewheel MOFs synthesized via SALE. Reprinted with permission from reference 99. Copyright © 2013 Journal of the American Chemical Society.

larger pore volumes than the original parent MOF. An additional expansion of these structures resulted in the creation of bio-MOF-103 ($Zn_8(ad)_4(tpdc)_6(OH)_2$) in which abdc was replaced with tpdc (6Å larger than ndc) as the linker in the MOF. It is of significance that neither bio-MOF-102 nor bio-MOF-103 can be synthesized by standard solvothermal methods.[108, 109] A recent example of SALE utilized in this manner is the SALEM-5 MOF series where the linker can be exchanged to create larger and larger MOFs, SALEM-6, SALEM-7, and SALEM-8.[89]

Stabilization of MOFs

One of the main drawbacks of using MOFs is the lower framework stability in comparison to other porous networks due to ligand lability. The varied ligand connectivity present in MOF frameworks, as well as diverse methods used to generate structures with improved stability will be explored in the following sections. The two most commonly seen connections at metal-ligand interfaces in MOFs are carboxylate based and N-heterocycle based. The high-valent metal-carboxylate frameworks and low-valent metal azolate frameworks usually show high chemical stability, which is in line with Pearson's hard-soft, acid-base (HSAB) principle.

Carboxylate based linkers

MOFs with carboxylate linkers make up a considerable proportion of known MOFs. MOF-5,[110] one of the most well-known MOF structures, was synthesized with 1,4-benzene dicarboxylate (BDC), a simple 4-coordinating organic linker. This deceivingly simple MOF was a significant breakthrough in the field due to its ability to retain its crystalline framework following evacuation of guest molecules. The incorporation of carboxylate groups as caps for the tetrahedral metal clusters allowed for previously unseen rigidity in the framework. The resulting $Zn_4(O)(CO_2)_6$ cluster is reminiscent of an existing zinc phosphate structure,[111] and bears significant similarity to naturally occurring zeolite structures. Following its discovery, MOF-5 has provided a basis from which many frameworks have been developed, most notably the IRMOF series reported by Yaghi and coworkers in 2002.[7] This IRMOF series (see isoreticular expansion for discussion) was developed using increasingly complex phenyl-based dicarboxylate linkers and the tetrahedral zinc clusters characteristic of MOF-5.

Phenyl carboxylates are a family of linkers that have been widely used in the synthesis of MOFs. This can be attributed to the ease of access to a variety of ligand sizes and geometries. Many carboxylate materials are commercially available or do not require a complicated synthetic process. Amongst these carboxylate ligands, the linkers can mainly be categorized by

topicity. The most common are ditopic, tritopic, and tetratopic ligands, with some extension into ligands with 6 or 8 carboxylate groups. While there have been MOFs that have been synthesized with monotopic formate ligands,[112] they are less prominent in the literature due to the low connectivity of the monotopic ligands, only connecting 2 metal clusters and forming 2-dimensional frameworks, resulting in high lability of the structure.

One of the most commonly used ditopic phenyl carboxylates is 1,4-benzene dicarboxylate (BDC), also known as terephthalic acid. A variety of MOF topologies are often initially synthesized with this ligand as a starting point for the development of an isoreticular series. This is because chemical reactivities between topologies are similar and the ideal range of synthetic conditions can be determined using this simple linker as a screening agent. Other than the IRMOF series developed by Yaghi and coworkers, the UiO series also employs the BDC ligand for the synthesis of UiO-66 and the subsequent UiO-67 and UiO-68,[113] which are synthesized with bi-phenyl-4,4'-dicarboxylic acid (BPDC) and terphenyl-4,4"-dicarboxylic acid (TPDC) respectively.

In MOF synthesis, one of the most challenging aspects is improving the chemical and thermal stability of the framework, especially in the absence of guest molecules. The inherent lability of the metal-ligand bonds is what allows for the formation of crystalline structures and allows for *in situ* defect correction. However, this is in counterpoint with the desire for high stability. Another concept that is often employed in the design and synthesis of MOFs is the hard-soft, acid-base theory (HSAB). This is reinforced by the high stability of zirconium-carboxylate type MOFs, a result of strong interactions between hard ions, Zr^{4+} and O^{2-} or OH^- ions to form the Zr-O clusters that make up the SBUs in most zirconium MOFs.

In recent years, there has been a significant interest in the synthesis and development of Zr-based MOFs. Simple synthetic pathways, high chemical and thermal stability and low toxicity have culminated in the push towards using these materials for practical applications. A significant step in the discovery of Zr-MOFs as a potential class of new material was the synthesis of UiO-66. UiO-66 was first reported by researchers at the University of Oslo, comprising of a $Zr_6(\mu_3\text{-}O)_4(\mu_3\text{-}OH)_4$ cluster as the SBU, with BDC as the connecting ligands. The discovery of this Zr-MOF launched many other research explorations into other Zr-carboxylate frameworks that would potentially possess similarly high stabilities. In general, MOF stability is complex and difficult to accurately predict. The metal-ligand bond strength is a key contributor to this, and it is highly dependent on the individual metals and ligands. In the case of Zr-O bonds within Zr-MOF structures, strong polarization and high charge density of the Zr^{4+} metal cation results in the strong affinity between Zr(IV) and the carboxylate oxygens.

Zr-MOFs demonstrate exceptional stability due to less labile coordination bonds. A major drawback of the lack of metal-ligand lability and resultant rapid bond formation is low crystallinity and irregular frameworks due to the material's inability to repair defects. One method developed to circumvent this issue is the introduction of modulating agents to the reaction mixture.

Stable MOFs with large pore sizes are highly desired for the incorporation of large functional groups or guest molecules. However, the incorporation of large linkers often results in a MOF that collapses upon solvent evacuation. In other cases, introduction of large linkers results in the formation of interpenetrated frameworks, which do not possess large pores and may even be non-porous. There have been many attempts to get around this issue by increasing the steric hindrance of ligands to prevent interpenetration or by using different synthetic conditions. With Zr-MOFs, using similar metal clusters has allowed for the synthesis of various MOFs using similar synthesis conditions due to the highly similar reactivities of most phenyl carboxylate groups with Zr-O clusters. Building upon the most well-known Zr-MOF, UiO-66, isoreticular expansion and topology-guided design have resulted in the vast library of Zr-MOFs afforded to us by literature today.

While a large proportion of carboxylate based MOFs are Zr-MOFs, there exist a multitude of other frameworks that incorporate different metals with carboxylate ligands. Most prominent in the field are the MIL series of MOFs, which includes but is not limited to MIL-101, a Cr^{3+}-terephthalate framework. The MIL series explores carboxylate based frameworks that coordinate to clusters varying from divalent to tetravalent metals. Within the MIL series, MIL-140 follows a series of tetravalent Zr-frameworks with increasing ligand lengths, forming an isoreticular series, MIL-140A, MIL-140B, MIL140C, and MIL-140D. Many of the other MIL-MOFs are formed with trivalent metal ions, commonly Fe^{3+} and Cr^{3+}, with some being extended to V^{3+}, Al^{3+}, In^{3+}, and Ga^{3+}.[114, 115]

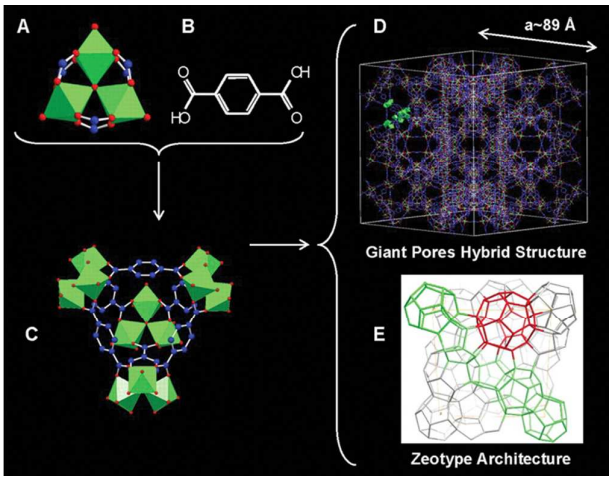

Fig. 8 A MOF with unusually large pore volumes and surface area that can be generated using various metal types through post-synthetic modification. Reprinted with permission from Reference 110. Copyright, © 2005 American Association for the Advancement of Science.

In 2014, Zhou and coworkers published a study with a series of MOFs synthesized from carboxylate ligands and Fe-based metal clusters. The theory proposed, kinetically tuned dimensional augmentation (KTDA), considers the rates of substitution of the linker, or bridging ligand, the modulator and coordinating solvent molecules. They employ preformed clusters, minimizing the potential for amorphous material as a result of the incomplete formation of metal clusters *in situ*. Preformation of metal clusters ensures that metal-ligand interactions are not kinetically competing with metal cluster formation. Acetic acid was used as the modulating agent in this study as it is compatible with the acetate moieties that form the metal clusters, reducing the number of variables in the carboxylate substitution process. From this study, it was noted that MOF crystallinity can be varied based on the modulator equivalence (with respect to the metal cluster). A deviation from the optimal amount of modulator to form a crystalline product resulted in the formation of non-crystalline products. It was observed that higher concentrations of modulator were required with increasing connectivity of both the ligand and the metal cluster. However, it cannot be said that there is a direct correlation between the connectivity numbers and the amount of modulator required as the ideal amount still varies across systems.[116]

N-heterocyclic based linkers

Unlike carboxylate-based linkers, N-heterocyclic based linkers are usually neutral in charge and lie on the other end of the HSAB spectrum. N-heterocyclic linkers or N-donor linkers are classified as a softer ligand, forming more stable interactions with softer metals such as Zn^{2+} or Ni^{2+} and other low valent metal cations. While these interactions are classified as soft, it does not imply lowered stability within the framework. In fact, there are N-heterocycle based MOFs that have chemical and thermal stabilities that are comparable to that of carboxylate-based MOFs. With the appropriate metal-ligand matching, frameworks can demonstrate high stability due to lower metal-ligand bond lability. One aspect in which N-heterocyclic based MOFs outshine carboxylate-based MOFs is in their stability in extreme pH conditions.

Amongst the many N-heterocycle based frameworks, a significant sub-class is Zeolitic Imidazolate Frameworks (ZIFs). As the name suggests, ZIFs possess structures similar to the class of aluminosilicate materials, zeolites. ZIFs mimic zeolites in terms of connectivity, with the metal-imidazole-metal geometry being comparable to that of the Si-O-Si geometry present in zeolites. However, with the rapid expansion of the MOF field, there currently exist ZIFs that possess geometric structures that are outside the typical zeolite topologies.[117, 118] ZIFs sit in the region between zeolites and MOFs, combining the advantages of both material classes. An interesting advantage of using ZIFs is the many synthetic methods that have been developed, allowing for the potential for many applications that might otherwise be unattainable due to the toxicity of organic solvents or harsh thermal conditions required in typical solvothermal synthesis. In addition to conventional solvothermal synthesis, alternative methods that have been explored are hydrothermal synthesis, ionothermal synthesis, sonochemical synthesis and solvent-free methods. The variety of available synthetic pathways has allowed for the development of interesting applications based on the mechanisms of seeding and crystal growth.[118]

One particularly useful application of ZIFs is in the immobilization of enzymes. A major obstacle in the useful biological applications of MOFs lies in the toxicity of MOFs and the solvents necessary for their synthesis. In addition, solvothermal conditions often require elevated temperatures and organic solvents, which are conditions that often result in decomposition or denaturation of useful biological species. The relatively mild synthetic conditions required for the synthesis of many ZIFs make them compatible for enzyme immobilization, fixing the enzyme conformation in the framework, allowing for increased activity compared to free enzymes. The framework also protects the enzyme from harsh conditions that might cause denaturation and can provide size selectivity of substrates.

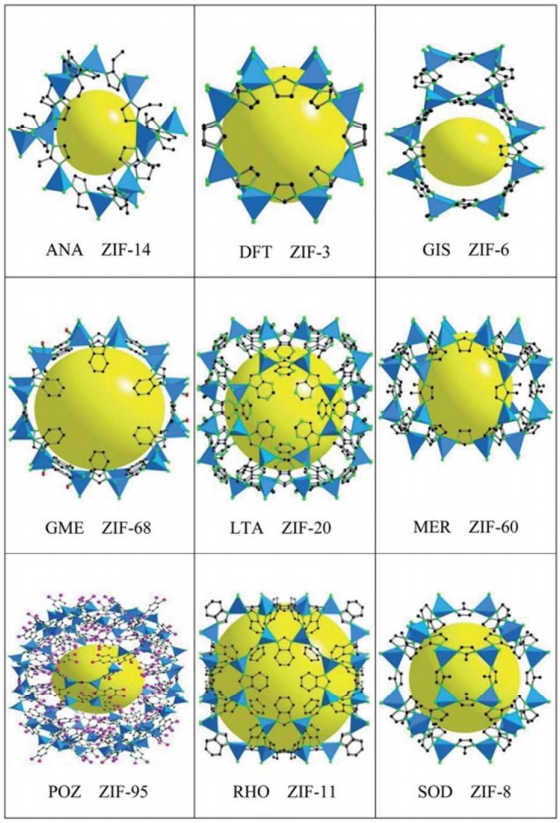

Fig. 9 Representation of various zeolitic imidazolate frameworks. Reprinted with permission from Reference 113. Copyright © 2014 The Royal Society of Chemistry.

Pyrazolates are N-heterocyclic groups that are similar to imidazoles, except with a smaller chelating angle of 70˚ instead of 145˚ and a shorter distance between the metal clusters in

the framework. In pyrazolate linkers, the coordination between linker and metal cluster is through the sp-hybridized N atom, as well as through hydrogen bonding of the adjacent N-H groups to the oxo-moieties that make up the metal cluster. In a fashion similar to that of carboxylate ligands, the spacer groups used between the coordinating pyrazolate groups can be varied, giving a range of geometries when combined with the multitude of available metal clusters. Amongst them, PCN-601 and PCN-602 are pyrazolate-based porphyrinic MOFs that demonstrate exceptional stability under highly alkaline conditions, maintaining porosity and crystallinity after treatment in saturated NaOH solution at 100˚C.[119, 120]

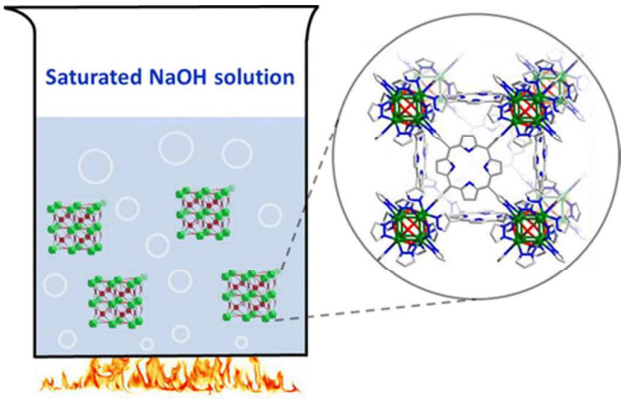

Fig. 10 Representation of extreme stability of Ni^{2+} pyrazolate MOFs in basic conditions. Reprinted with permission from Reference 114. Copyright © 2016 Journal of the American Chemical Society.

Multicomponent MOFs

Synthetic strategies for multicomponent MOFs

The successful synthesis of multivariate Metal-Organic Frameworks (MTV-MOFs), a class of MOFs that contain a vast array of possible components within their structures, has attracted great interest in recent years. This interest primarily stems from the desire to fine-tune and control the internal environment and related properties of MTV-MOFs for use in gas storage, gas separation, and cooperative or tandem catalysis.

Mixed-linker MOFs

A major subclass of MTV-MOFs is mixed-linker MOFs. Mixed-linker MOFs are highly desired because they offer a unique approach to MOF functionalization. Using these systems, pore environments and structural defects can be selectively generated by linkers that can be either inserted or removed to achieve a desired functionality. To achieve this vast array of possible functionalities, mixed-linkers with different lengths and different geometries are often incorporated in the framework in an ordered or disorder manner during the facile one-pot synthesis or through postsynthetic modification.

In 2010, an early example of mixed-linker MOFs was reported by Yaghi and coworkers. In their study, they reported a series of MTV-MOF-5 with linkers bearing approximately the same lengths but that contained different functionalities.[121] In their study, they incorporated eight distinctive functionalities: $-NH_2$, $-NO_2$, -Br, $-Cl_2$, $-(CH_3)_2$, $-(OC_3H_5)_2$, $-C_4H_4$, and $-(OC_7H_7)_2$ into their framework. These functionalities were immobilized into a singular crystalline network but had a disordered distribution throughout an ordered framework. This resulted in a 400% enhancement in the MOF's selectivity for carbon dioxide over carbon monoxide. A recent notable work with mixed-linker MOFs was done by the Zhou group. This group reported the one-pot synthesis of a UiO-66 based multivariate MOF, where the topologically distinct linkers, 2-connected BDC and 4-connected TCPP, were incorporated into the ultra-stable UiO-66 backbone. Their study, like the study conducted by Yaghi and coworkers, also resulted in a disordered distribution of the linkers into an ordered structure.[122]

Although there are many advantages to using mixed-linker MOFs, targeted linker incorporation still poses a significant challenge. The metals within a cluster can play a role in linker positioning in a mixed linker system. MOFs are thermodynamically driven supramolecular assembly products. From a thermodynamic perspective, some metal clusters can favor a specific linker conformation, allowing for a semblance of control in the linker positioning within a mixed-linker MOF. Using traditional synthetic methods, it is difficult to synthesize a fully connected MOF without any defects using a single linker. However, a fully connected mixed-linker MOF, can be generated from the combination of two or more linkers, a result of thermodynamic favorability, but can lead to disorder within the structure.[123] The design and placement of linkers to limit the disorder within the structure is essential in order to achieve pre-designed properties in the mixed-linker MOF, and has been a major focus of study in recent years.

An example of a successful ordered linker placement strategy with mixed-linkers was demonstrated by Tefel and coworkers.[124] In their strategy, a series of mixed-linker Zn-MOFs were synthesized in a modular quaternary system. Three topologically distinct linkers were then introduced into the preformed highly porous quaternary MOF from the first step. By further varying the functional groups on the organic linkers, eight isoreticular frameworks were obtained with ordered pore architectures. This strategy, based on topologically distinct linkers, resulted in a new synthetic avenue that has since been incorporated in the synthesis of many multivariate MOFs. For example, this strategy has been used for MOFs such as PCN-133 and PCN-134.

Many new mixed-linker MOFs are discovered using traditional solvothermal one-pot synthesis techniques such as the ones used by Tefel and coworkers. However, for this approach, a major drawback is that one-pot synthesis requires precisely controlled solvothermal conditions. When these reactions are not controlled, multiple undesired phases or products can easily form. From this perspective, post-synthetic modification

methods are more suitable for the controllable design of mixed-linker MOFs. One of the widely used strategies that uses post-synthetic modification is linker exchange, which was discussed in section 2.4.5. As this technique utilizes the reversible nature of metal-ligand bonds, it has become extremely useful for ordered mixed-linker MOF synthesis.[63] This method involves the synthesis of structures under mild conditions, giving structures that cannot be synthesized via traditional solvothermal methods.

Another strategy to produce mixed-linker MOFs through post-synthetic modification is through linker installation. This method uses coordinatively unsaturated metal clusters and can be utilized to engineer pore environments with precisely placed functionalities.[52, 125] This strategy was developed by the Zhou group using a zirconium MOF, PCN-700. PCN-700 is a stable MOF with coordinatively unsaturated Zr_6 metal clusters. This unsaturation is vital for the introduction of new linkers with varied lengths and functionalities. A variety of different linkers were installed into the parent PCN-700 using linker installation, resulting in 11 new daughter MOFs. Each new MOF was highly ordered and contained up to three distinctive functional groups.[52, 125] Recently, Zhou and coworkers reported a general method, linker thermolysis, to selectively remove thermolabile linkers in MTV-MOFs.[126] This approach was achieved by utilizing the relationship between linker spatial distribution in MTV-MOFs and vacancy apportionment in hierarchically porous MOFs after the thermolabile linkers were removed from the framework. Mimicking biological methods by selectively removing individuals from integrated systems, linker thermolysis provides fresh insights into deciphering unit apportionment in multivariate materials.

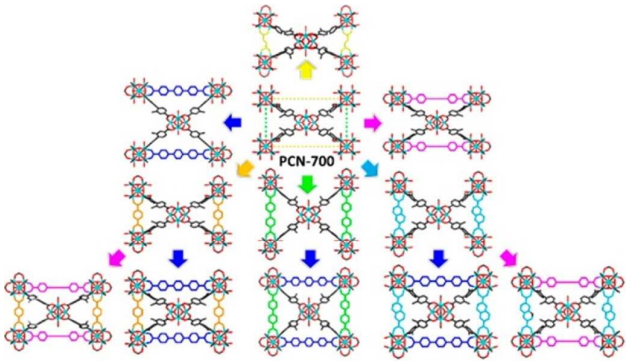

Fig. 11 Single-crystal structures of PCN-700 and its daughter MOF derivatives viewed along the *a*-axis. Reprinted with permission from Reference 52. Copyright 2017 Journal of the American Chemical Society.

Mixed-metal MOFs

Mixed-metal MOFs are also a major subclass of MTV-MOFs. As the name suggests, this subclass contains more than two kinds of metal species in a single metal cluster. These types of MOF clusters are rare as solvothermal synthesis usually produces mixed MOF phases rather than a pure mixed-metal MOF. In 2014, Yaghi and coworkers reported a series of microcrystalline MOF-74 where every MOF variant in the series contained divalent metal clusters (Mg, Ca, Sr, Ba, Mn, Fe, Co, Ni, Zn, and Cd) and were obtained through one-pot solvothermal reactions.[127] Energy-dispersive X-ray spectroscopy suggests that the metal ions are heterogeneously arranged within each crystalline MOF sample.

After the first report in 2014, other successful strategies have been employed to achieve mixed-metal MOFs.

Through later studies, it became possible to decipher the spatial distribution of metal in a mixed-metal MOF. A study done by Qi and coworkers used $(M_3O)_2(TCPP\text{-}M)_3$, where M refers to Mn, Fe, Ni, Co, and Mg.[128] The arrangement of the mixed metals inside of the framework were determined by the use of x-ray photoelectron spectroscopy (XPS), ultraviolet visible spectroscopy (UV–Vis), and diffuse reflectance spectroscopy (DRS). Through these techniques, it was found that mixed-metal MOFs can exist as either domain or well-mixed structures. Domain, in this case, refers to two or more distinct metal clusters in a MOF where only one type of metal exists in each cluster. Conversely, a well-mixed structure is a MOF where the clusters contain two or more metals per cluster. Well-mixed clusters are rarer than domain type clusters.

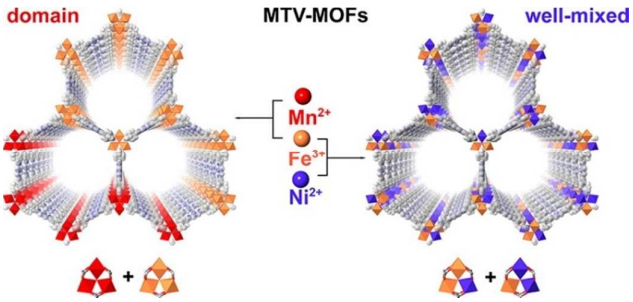

Fig. 12 Mixed-metal PCN-600 derivatives with different metal combinations. Metal distribution in mixed-metal PCN-600(Mn/Fe) demonstrate the domain arrangement while metal distribution in mixed-metal PCN-600(Ni/Fe) demonstrate the well-mixed arrangement. Reprinted with permission from Reference 122. Copyright © 2016 Journal of the American Chemical Society.

Similar to what we observe in mixed-linker MOFs, it is possible to form mixed-metal MOFs through post-synthetic modification, (see section 2.4.2). A recent example of a well-mixed cluster that was formed through post-synthetic modification was done by Zhou and coworkers in PCN-700. [129] Well-mixed type clusters were formed without destroying the parent structure and was achieved through a single-crystal to single-crystal transformation mechanism. Interestingly, it was shown that part of the stability of this new structure was from a ligand migration. The ligands in this structure migrated from the original metal in the cluster to the new metal once the metal had been incorporated into the cluster structure. This cooperative cluster metalation and ligand migration lead to the formation of bimetallic MOFs with decanuclear Zr_6M_4 (M=Ni, Co) clusters from the parent hexanuclear structure. This transformation occurs through the μ_3-OH and terminal

H_2O ligands on the original $[Zr_6O_4(OH)_8(H_2O)_4]$ cluster. These ligands reacted with the M^{2+}, forming the bimetallic $[Zr_6M_4O_8(OH)_8(H_2O)_8]$ cluster and assisting formation of the ligand migration. [129]

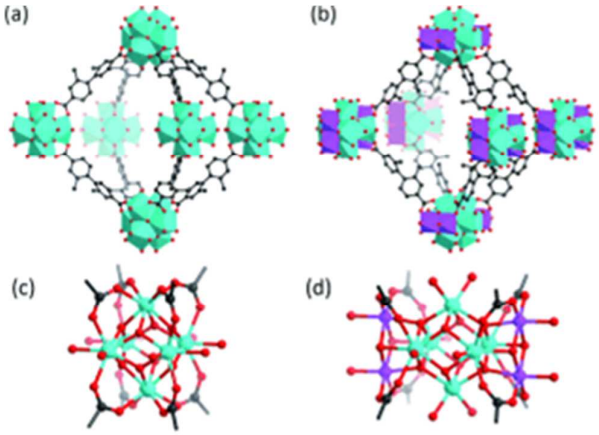

Fig. 13 a) and b) The structure of PCN-700 and PCN-800(Ni); c) and d) the Zr_6 cluster in PCN-700 and the Zr_6Ni_4 cluster in PCN-800(Ni). Reprinted with permission from reference 123. Copyright © 2017 Angewandte Chemie.

Defects in MOFs and Hierarchically Porous MOFs

Formation and Characterization of Defects in MOFs

In recent years there has been a greater emphasis on the understanding of how defects in MOFs can be created, tuned, or prevented Defects in particular have given researchers the ability to control the pore size, pore volume, and surface area of specific MOF topologies while retaining the chemical and physical properties of the original material.[10, 73, 130-134] Defects in MOF's are defined as sites (e.g. linkers, nodes, clusters(**reo**)) that break the regular periodic arrangement of the framework due to missing or modified SBU's. From this definition two systems of defects are formed: inherent defects and engineered defects.[134-138]

Inherent defects arise from the relatively immobile nature of atoms or molecules in solid networks. During the crystal growth process, labile linkers result in reversible bonding. However, as a network forms, some defects do occur within the structure. When a defect occurs, it can be extremely difficult for missing connections or dislocations to repair themselves. These defects form without any further modification of the parent framework. An example of the difficulty of inherent defects in a MOF can be demonstrated with the structure of UiO-66. UiO-66 is a MOF that is created by the incorporation of 12 connected $[Zr_6O_4OH_4]$ clusters and homoleptic benzenedicarboxylate (BDC) organic linkers. It has been estimated that up to 25% of linkers per cluster could be inherently missing in UiO-66, even when following standard synthetic conditions.[139] Thermogramavetric analysis (TGA) was used in this study to demonstrate this inherent missing linker aspect of UiO-66.[139] Several other studies have shown that lower thermal stabilities are expected for defect-rich MOFs in comparison with their non-defective parent frameworks.[134, 140, 141]

The second system of defects in MOF's are called engineered defects. Engineered defects are defined as the intentional variation of synthetic conditions (e.g. time, temperature, pressure), reactant identity (e.g. addition of fragmented ligands/nodes, templating agents), stoichiometric ratios of reactants (e.g. ratio of metal nodes to ligands), addition of modulating agents (e.g. Acetic Acid), or post-synthetic techniques (e.g. acid/base treatment, thermal treatment) with the purpose of creating defects in the structure. In order to further investigate the formation of defects, all defect forming procedures (inherent or engineered) can be classified into two classes: *de novo* synthetic techniques and post-synthetic techniques.

De novo synthetic techniques refer to a variation in the synthetic conditions that creates deviations (defects) from the parent framework.[134] For example, the type and number of defects that are created has a major dependence on modulator identity and concentration. Zhao and coworkers compared three different modulators, trifluoroacetic acid (TFA), formic acid (FA), and acetic acid (AA) and their relative effects on defect formation in UiO-66. The conclusion of this study was that the higher the pKa of the modulator used, the higher the defect concentration.[142] In addition to pKa, a useful comparison can be made between non-coordinating modulators, such as hydrochloric acid (HCl), methanol (MeOH), and amino acids, and coordinating modulators such as TFA, AA, and benzoic acid (BA).[142] Weakly coordinating modulators should be used to create missing linker defects while coordinating modulators should be used to create missing cluster (reo) defects.[58, 136, 142-146] For defect formation, the concentration of a chosen modulator is just as important as the chemical properties of the modulator. An example using UiO-66 uses acetic acid as a modulator during synthesis. By utilizing a range of concentrations of the modulator, the concentration of missing linker defects can be precisely tuned as shown in Figure 15.[145]

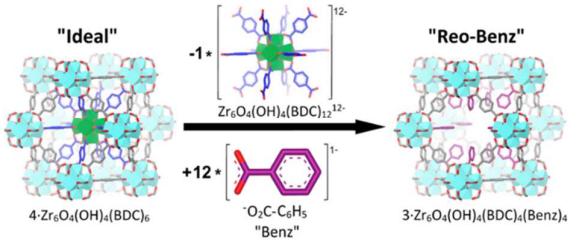

Fig. 14 Cluster/reo-type defect formation using a benzoic acid modulator. Reprinted with permission from reference 138. Copyright © 2017 Journal of the American Chemical Society.

Recently, new methods of modulation have been developed, producing MOF nanoparticles with missing linker defects and high surface areas. This method uses Ionic Liquids (IL) to prepare pre-formed MOF clusters. These pre-formed clusters can be used to tune defects in UiO-66.[147] However, defect creation and
tunability is not limited to the use of modulators. In the UiO-66 family, lowering the synthesis temperature, the BDC:Zr ratio, or

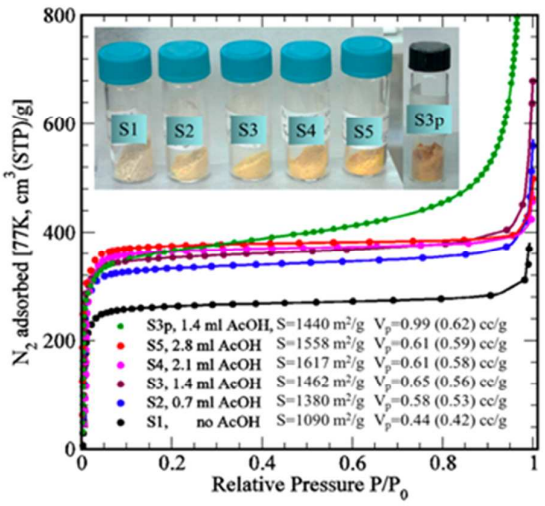

Fig. 15 Various concentrations of acetic acid modulator and its effect on defect formation. Reprinted with permission from reference 139. Copyright © 2017 Journal of the American Chemical Society.

the reaction time can shift the solution equilibrium away from the formation of the BDC-Zr bonds. A shifting away from equilibrium can aid the formation of linker or reo type defects.[145, 148] These defects can be induced by the addition of a secondary linker that possesses a chemical structure similar to the bridging ligand. This synthetic variation was tested with samples of HKUST-1 and it was demonstrated that the percentage of defects in the final structure was dependent on the concentration of isophthalic acid derivatives introduced into the reaction mixture, giving framework defects of up to 8%.[149]

Another technique that has been used in defect creation in MOFs is post-synthetic modification. These techniques are defined as procedures that modify the parent framework following the initial synthesis.[134, 150] These techniques include but are not limited to: solvent exchange, thermal treatment, and acid/base etching. For solvent exchange, the concentration of linker defects is proportional to the increased duration of treatment. A common solvent used in solvent exchange is methanol, which can displace the reaction solvent.[151] Thermal treatment of frameworks can also induce defect formation. A recent report on thermally induced defect formation in MOF-5 indicated that heating the structure to temperature between the activation and decomposition temperatures induced *in situ* decarboxylation of the linker fragments.[152] Etching has also been known to create defects in MOFs and often uses aqueous solutions of varying pH.[153-155] An example of defect formation using the etching technique utilized a defective sample of UiO-66 produced using the modulated synthesis technique, followed with treatment in an aqueous solution containing HCl. This removed the benzoic acid modulators from the framework, in turn creating new defects in the structure.[156, 157] Another example of etching was demonstrated with MIL-100(Fe). In this study, the MOF was treated with solutions containing TFA or $HClO_4$, inducing defect formation by substitution or removal of the 1,3,5-benzene tricarboxylate (BTC) linkers.[148]

Various well-known techniques for defect development in MOFs have been paired with theoretical calculations in order to study how the defects may affect the chemical and physical properties of the material. It must be understood that the characterization of defects requires the use of multiple techniques. Understanding defects in metal-organic frameworks is still considered a young area in the field and existing literature is not comprehensive. Characterization methods, DFT, and other theoretical calculations have all previously been shown to be effective in the understanding of defects. Many new tools can be paired with these methods to give the best insight into MOF structure and functionality. This combination of new and old techniques has been quintessential in the further understanding of tenable defect formation.[139, 158, 159] For an overview of the techniques used in defect characterization as well as standard MOF characterization, see Section 7.

Synthesis of hierarchically porous MOFs

Hierarchically Porous Metal-Organic Frameworks (HP-MOFs) contain engineered mesopores/macropores in addition to the inherent micropores associated with that specific framework. HP-MOFs integrate the dual merits associated with mesoporosity and microporosity, helping to mitigate the pitfalls associated with each. While the micropores contribute to the bulk of the surface area of a material, the mesopores and macropores provide the accessibility to gases and larger molecules that is desirable in many applications. The larger pores assist in many applications as they allow molecules to quickly diffuse through large crystal particles to reach the storage or reactive sites that may be contained within the micropores of the structure. The large surface area paired with tenable mesopores allow for a new class of metal-organic frameworks to be designed for specific functions in separations, catalysis, photochemistry, and drug delivery.[160-163]

Although there is immense potential for hierarchically porous MOFs various areas, only a few methods have been reported demonstrating the extraordinary defect creation control that is necessary for generating HP-MOFs. These techniques that have thus far been reported include template-based synthesis,

modulator-based synthesis, perturbation-assisted synthesis, ligand fragmentation, and linker labilization.

Templated Synthesis

Templated Synthesis has been used for decades in many areas of materials synthesis, but only recently has it been applied to the synthesis of metal-organic frameworks. In the templated synthesis technique there are two main categories of templating agents. The first category is templating agents that are cationic, and the second category is templating agents that are anionic/coordinating.

One of the first examples of the templating technique in MOFs was in 2008. Qiu and coworkers created a hierarchically porous version of HKUST-1 using CTAB as a templating agent. CTAB was selected in this study as it is a well-known cationic surfactant.[164]

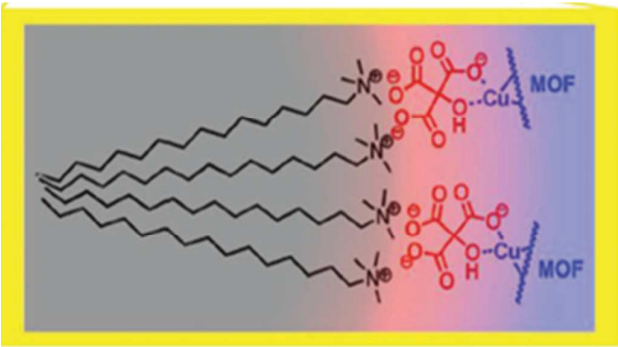

Fig. 16 Representation of aggregation formation of templating agents used in MOF synthesis. Reprinted with permission from reference 144. Copyright © 2011 Journal of the American Chemical Society.

It was found that during the templated synthesis of HP-MOF's, the templating agents tend to form aggregates as shown in Figure 16. Evidence then suggested that the mesopore diameter was strongly dependent on the hydrophobic volume of these self-assembled aggregates.[163, 164] Following this breakthrough, a general mechanism of defect formation using templates was hypothesized based on these results. Since 2008 many advances in template based synthetic techniques have been made. One of these advances include the use of CTAB paired with co-templates such as 1,3,5-Trimethylbenzene (TMB) or Citric Acid (CA).[164, 165] An example of co-templates used in MOF synthesis is the addition TMB as a co-template with CTAB in HKUST-1, generating a series of swelled aggregates, increasing the mesopore size from 5.6 to 31.0 nm.[164] A second major advance in templated synthesis of HP-MOFs was made when neutral templating agents such as block co-polymers were investigated. The block copolymers employed as templates are often of the Pluronic® type, which are generally composed of ethylene oxide (EO) or propylene oxide (PO).[163] One example reported the use of P123 and F127 as templates in the synthesis of HP-MIL-53. The mesoporous structure generated in this system resulted in two distinct mesoporous systems. The first system contained a mesopore size of around 4.0 nm. The second system contained mesopore sizes that ranged between 5.4 and 7.6 nm.[166]

In addition to cationic templating, anionic and coordinating templates have also been shown to be of importance in this field. A recently developed technique called modulator-induced hierarchal defect formation combines the concepts of both; basic defect formation using small coordinating modulators such as TFA, BA, and FA. This combination aims at using larger chain templating agents to yield size control over the mesopore system. In 2017, Guorui Cai and Hai-Long Jiang reported the use of long-chain carboxylic acids as coordinating templating agents in order to generate HP-MOFs with tenable

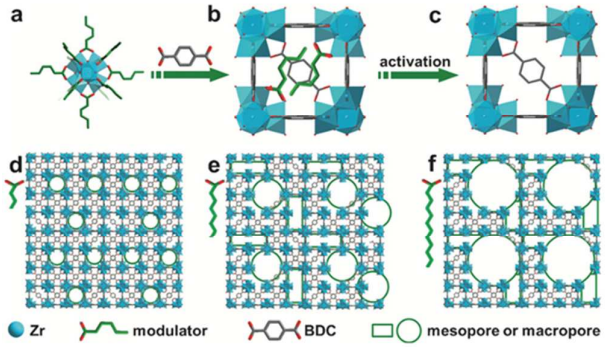

sizes of mesopores. HP-UiO-66 can be generated with controlled mesopore sizes up to 8.6 nm.[167] This method has also been reported to be successful in other MOF systems such as MIL-53, DUT-5, MOF-808, and MOF-5.[162, 168]

Fig. 17 Modulator-induced hierarchical defect formation. Reprinted with permission from reference 163. Copyright © 2017 Journal of the American Chemical Society.

Linker Fragment Co-Assembly

A different approach that has been recently developed for the synthesis of HP-MOFs is called ligand fragment co-assembly (LFCA). This method was developed by Zhou and coworkers in the study of defect formation in the PCN-125. LFCA shown in Figure 5, utilizes two types of ligands, the primary ligand and its ligand fragment. During synthesis, the ligand and its fragment crystalize into the same framework, creating linker based defects. In their study of PCN-125, it was found that isophthalate derivatives must be used as the fragments in order to generate controllable mesopore sizes and ratios. The exact size and ratio of the mesopores was dependent upon the identity of the isophthalate derivative as well as the ratio of the linker and its fragments. [169] The LFCA method has been shown to be extremely useful for studies of PCN-125. Since its initial use, LFCA has also been demonstrated in many other MOF systems: UiO-66,[170] NU-125,[149] MOF-74,[171] and HKUST-1.[172] The versatility of LFCA lies not only in its ability to tune the mesopore to micropore ratio through fragment concertation variations, but also in its ability to change the size and chemical environment of the mesopore through changing the identity of the fragment.[144, 149, 168, 171, 173] It is for this

second reason that the LFCA technique has been shown to be a unique way to introduce various functional groups into a framework.

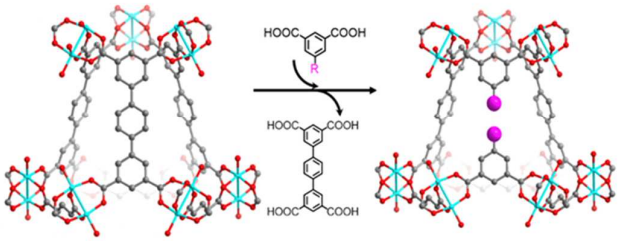

Fig. 18 Ligand fragment co-assembly in PCN-125. Reprinted with permission from reference 165. Copyright © 2012 Journal of the American Chemical Society.

Linker Labilization

In 2016, Zhou and coworkers also reported a second technique for producing HP-MOFs called linker labilization (LL). This strategy was inspired by methods such as linker installation,[126, 174] solvent assisted ligand exchange (SALE), and solvent assisted linker incorporation (SALI).[175, 176] Linker labilization is a technique that incorporates labile linkers into the framework followed by subsequently labilizing and removing these linkers by splitting them into two, removable, mono-carboxylate fragments under acidic conditions. This was first seen in a UiO type MOF structure, PCN-160. PCN-160 can be generated from Zr clusters and an azobenzene-4,4'-dicarboxylate (AZDC) linker. AZDC can be incorporated up to 43% while maintaining stability in the structure after the LL process. By using AZDC as the labile ligand along with various concentrations of acetic acid as the labilizing source, the pore size could be tuned from 1.5 to 18 nm. This process was also tested on CYCU-3, an aluminum based MOF, generating a hierarchically porous framework.[161, 177] Very recently, Zhou and coworkers expanded this linker labilization into a series of ultrastable MOFs, in order to obtain more stable HP-MOFs.[126] Here, linker thermolysis, a thermal induced linker labilization approach, has been proved useful for constructing hierarchical pores inside UiO-66, MIL-53, MOF-5 and MIL-125. Meanwhile, metal oxides were created during the linker thermolysis, possibly due to the formation of thermolabile linker domain inside the structures. These methods mentioned above led to HP-MOFs with high stability and single crystallinity, which would be very difficult to achieve by other methods.

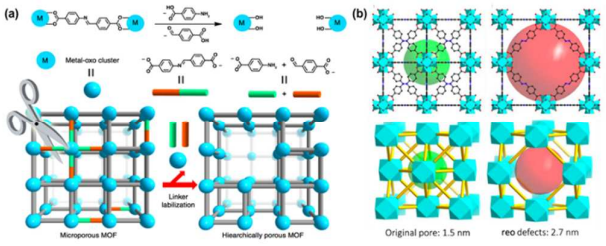

Fig. 19 Linker labilization scheme and visualization of reo defects in MOFs. Reprinted with permission from reference 156. Copyright © 2017, Rights Managed by Nature Publishing Group.

Perturbation-assisted nano-fusion

Another technique with the ability to generate HP-MOFs and controllably maintaining the pore size and ratio of the final product is called perturbation-assisted nano-fusion (PNF). The main concept that sets PNF apart from the other techniques discussed is that this method is based in the use of SBUs that are generated during synthesis but that do not assemble into large single crystals. This technique allows for further aggregation of these SBU's into nano-sized MOF particles, in which the scaffolding of the framework can be completed. MOF crystals can then be embedded in an amorphous matrix using a nano-fusion mechanism, resulting in spontaneously formed mesopores. The size and nature of these pores can be controlled by tuning the speed of crystallization and nano-fusion growth. The choice in solvent or the stirring rate of the reaction has been shown to control the speed of crystallization in these systems. However, the tuning of the nano-fusion growth in this system is much more complex than previous methods and is still not fully understood. Current understanding involves tuning the supramolecular interactions of the nano-sized MOF particles formed before nano-fusion occurs. The supramolecular interactions that have been studies thus far include hydrogen bonding and π–π stacking. A few examples of the use of PNF in MOF synthesis are the synthesis of MOF-74, IRMOF-3, Cu-BDC, and Cu-BTEC all of which showed controllable mesoporous structures in the final respective MOF products.[178, 179]

Applications of MOFs containing defects

As seen in section 5.2, using a variety of methods, the ability to design and tune hierarchically porous metal-organic frameworks has been a recent research hotspot. The combined efforts of many research groups have led to the practical use of hierarchically porous MOF uses in a variety of applications. Although MOFs have already demonstrated significant applicability in many fields, such as gas adsorption, small molecule separations, catalysis, and chemical sensing, there is still a great deal of untapped potential for applications in MOFs. Defect engineering has emerged as one of the leading approaches to further tune the properties of MOF's through defect creation or mitigation.[133, 134, 137, 138, 180, 181] In adsorption and separation based applications, the selective

chemical and physical interactions of guest molecules within the structures of a framework can be tuned, enhancing the performance of the MOF in this field. Improving a MOF's selectivity for CO_2 through defect engineering has been reported on many occasions. Specifically, defective PCN-160, HKUST-1, and NU-125 synthesized using the LFCA method have all shown improved selectivity of CO_2 over other gases, particularly N_2, H_2, and CH_4.[149, 169] A second example of a remarkably enhanced CO_2 uptake can be seen in defective MOF-5. The defects in this study were created by thermal treatment and were shown to have enhanced the CO_2 uptake 120% from 0.8 mmol/g to 2 mmol/g.[152] Another example of this selective guest molecule capture can be seen in defective MIL-53, where the heat of adsorption of ethylene (C_2H_4) in the structure is increased to 25.5 kJ/mol, compared to 19.3 kJ/mol in the non-defective structure. This increased heat of adsorption was shown to result in a significant increase in uptake capacity when compared to the non-defective framework.[182]

A recent report by Hupp and coworkers in 2015 is an example of the versatility of defective MOFs. Their study focused heavily on defective UiO-66 and involved the incorporation of free carboxylic acids into the framework. This strategy was effective for the sequestration of a broad range of toxic chemicals. One of the major reasons for the sequestration effectiveness that was exhibited by this MOF is found within the MOF backbone. The increased capacity for NH_3 exhibited by the MOF was due to an acid/base interaction with the carboxylic acid groups. The increased capacities for SO_2 and NO_2 was due to the reactive capabilities of the carboxylic acids.[181] After this initial work by Hupp and coworkers, Zhou and coworkers were able to demonstrate that the chemical functionality of the ligand fragments could be altered for gas selectivity tuning by using the LFCA method.[169] Additionally, work with UiO-66 done by Chen and coworkers reported that defect creation using acetic acid modulation increased the defective UiO-66's adsorption of dichloromethane (DCM) by 47.3%. All three examples demonstrate how tuning the chemical environment and creating defects can be used to tailor MOF's for specific applications.

The main characteristics that are highly tenable by defect engineering in hierarchally porous MOFs are: pore sizes, surface areas, and window size. The multiple, mixed levels of pores present in HP-MOFs have enabled this class of MOF to obtain remarkable loading capacities, diffusion coefficients, and optical properties. One such example of the possible uses of HP-MOFs is in a dye adsorption experiment using HP-MIL-101. In this experiment, it HP-MIL-101 exhibited remarkably accelerated adsorption and desorption kinetics in comparison with ideal MIL-101 crystals. The accelerated kinetics of this system is of particular interest for the development of MOFs for a dye-sensitized solar cells (DSSC).[183] A second example was reported for the investigating HP-IRMOF-3. The HP-IRMOF-3 structure enabled the simultaneous confinement of multiple large molecular dyes such as Rhodamine B. The MOF in this study exhibited the fluorescent properties from the dye encapsulated within its pores. This structure was still able to have open pore spaces for diffusion of other guest molecules while dyes were also encapsulated.[178]

Another application for defective MOFs is ion mobility and channeling. A report from 2015 detailed how linker defects in HP-UiO-66 increased the level of proton conductivity by nearly 3 orders of magnitude over a non-defective UiO-66. The Lewis acid sites formed as a result of the ligand defects provide a source of "mobile" protons while the increased pore size in the defective structure yields a pathway for increased proton mobility and diffusion.[184] Defects generated in a Ni based MOF through post-synthetic treatment with KOH, also yielded enhanced ion mobility. This Ni based MOF had a defective framework with a 4x enhancement of hydroxide ion conductivity as compared to known hydroxide ion conductors. The authors of this study, Navarro and coworkers, hypothesized that as a result of the enhanced mobility, this defective Ni-based MOF could be integrated into alkaline polymer electrolyte fuel cells (APEFC).[154]

Metal-organic frameworks and porous materials have been studied for their applications in catalysis for many years. However, the recent knowledge gained from defect engineering in MOF has provided a new way to increase catalytic turnover ratios, enhancing the selectivity. These factors have helped MOFs to obtain higher yields and has resulted in the development of highly advantageous solid-state catalysts. The mesopores within the HP-MOF structure form windows on the walls of the channels, allowing for a more efficient substrate diffusion between neighboring channels. Therefore, the substrates can reach the active sites much more efficiently than in a non-defective MOF.[134, 137, 157, 160, 161, 170, 185-187]

Tuning the Lewis acidity of the active site has also been explored in recent work. The Hirshfeld-electron charge of the active Zr sites in UiO-66 can be directly measured and can effectively be tuned using defects. The higher the Hirshfeld-electron charge, the lower the activation energy for the reaction, thus resulting in higher activities at the active site.[136] As seen in this UiO-66 example, changing the modulator or functionalizable ligand fragments changes the activity and number of the active sites through defect formation. The ability to provide solid state supports for homogeneous catalysts improves the activity and cyclability of the material. This remarkable correlation was established while investigating the cyclization of citronellal to form isopulegol.[136]

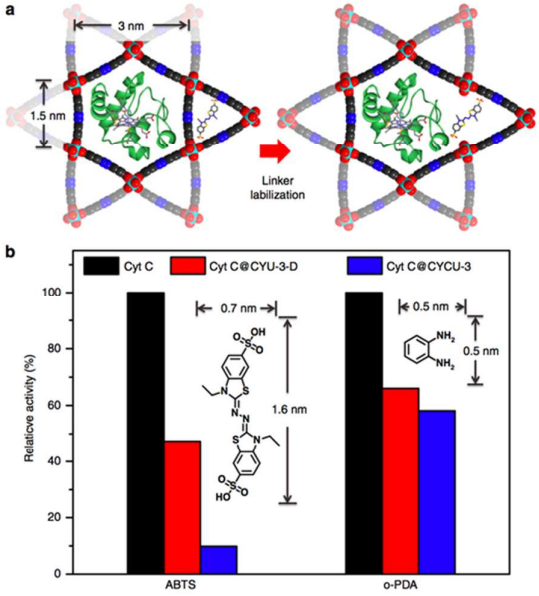

Fig. 20 Activity of HP-CYCU-3 vs. non-defective CYCU-3. Reprinted with permission from reference 156. Copyright © 2017, Rights Managed by Nature Publishing Group.

Bridging the use of defective MOFs in catalysis and biological applications can be seen through an example that was reported Zhou and coworkers. As shown in Figure 20, HP-CYCU-3 yields a major increase in the enzymatic activity over ideal CYCU-3 in the oxidation reaction of ABTS.[161] This phenomena was also seen in PCN-600 and NU-1000.

Although defects have been used in remarkable advancements and applications in the MOF field, not all applications in the MOF field benefit from defects. This is demonstrated in a study of MOF-5 and its hydrogen storage applications, where defective MOF-5 yielded a lower uptake capacity.[188] Understanding what causes defects and how defects are generated also provides vital insight into the process of MOF formation, allowing a more intimate understanding of this class of materials. Through understanding defect creation along with what synthetic conditions led to specific structures, defect chemistry can lead to breakthroughs in the manipulation of conditions to obtain desired structural characteristics in MOFs.

Synthesis and Application of MOF composites

As previously described in the above sections, Metal-Organic Frameworks (MOFs) are a class of materials showing amazing potential in fields such as gas storage,[189, 190] separations,[132] catalysis,[191] and many more.[132, 154, 191-194] A significant amount of the recent progress in generating practical applications for MOFs can be attributed to the controllable integration of MOFs with other functional materials.[195-197] These new materials, Metal-Organic Framework Composites, have been successfully generated through MOF integration with metal nanoparticles, both organic and inorganic oxides, quantum dots, polymers, various carbon-based materials, enzymes, silicon based materials, and even polyoxometalates. This section will describe the synthetic techniques used to generate three specific groups of these composite materials and their applications.[195, 198-204]

MOF-Polymer Composites

The first type of materials that will be discussed is MOF-Polymer composites. The number of papers published per year regarding the hybridization of polymers and MOFs has exponentially increased since 2005, when there was only one publication on MOF-polymer composites, to 2016, when there were 289 publications.[205] MOF-polymer composites can be separated into three main categories: Polymer@MOFs, MOFs@Polymer and polyMOFs.[196]

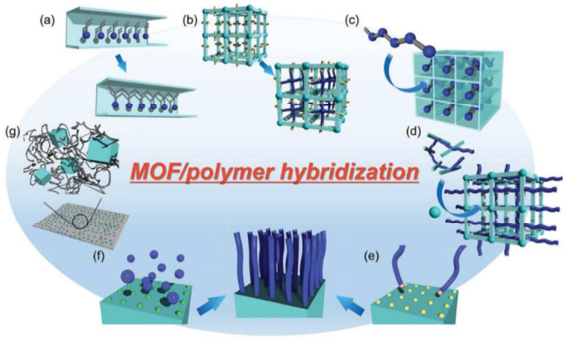

Fig. 21 Schematic Illustration showing various types of MOF-Polymer Composites. Reprinted with permission from reference 192. Copyright © 2017 Journal of Chemical Engineering.

Polymer@MOFs and MOFs@Polymers

The first two categories of MOF-polymer composites are quite similar in their description. Polymers@MOFs are defined as composite materials resulting from the inclusion/growth of a polymer inside or on the surface of a MOF. In contrast, MOFs@polymers are defined as the growth of a MOF inside or on the surface of a polymer. Not only is the identity of each component important but the generated structure type has a significant impact on the possible applications of a composite. For further classification, both composite categories can be further separated into three different structure types. These structures include composites generated by amorphously mixing the components (i.e. mixed fibers), composites generated by functionalizing the surface of one component with another (i.e. Core Shell Structures), and composites where one component is contained in the pores of the other component. Composites generated by amorphously mixing the two components have shown great promise in advanced gas storage and separation applications.[131, 195-197, 206] A composite between of MIL-53 or UiO-66 and cellulose acetate (CA), yields a functional composite for the selective adsorption of sulfur odorant compounds from pipeline natural gas. Some other examples include a polyamine/MIL-101(Cr) composite material that shows extremely high selectivity for CO_2 over N_2[207] and a UiO-66/polyurethane composite that was proven to be an extremely improved sorbent for the adsorption of benzene and n-hexane.[208]

In recent years, composites generated by functionalizing the surface of one component with another has become of major interest within chemistry, especially for biological applications. For example, a MOF@polymer core-shell structure was created by coating small UiO-66 crystals with BDP-imine. BDP-imine is a luminescent biocompatible polymer. The resulting properties of the composite material such as low cytotoxicity, small and uniform particle sizes, improved luminescence, and even a well-retained pore integrity make this composite a strong candidate for bio-imaging and enhanced cellular uptake

applications.[209] The last structure type described above is a composite where one component is contained in the pores of the other component. These structure types generally combine the chemical properties of one component with the physical properties of the other. For example, Wang and coworkers developed a polymer@MOF composite of ZIF-67 and polyaniline (PANI). Their composite was generated by first synthesizing ZIF-67 using traditional methods, followed by an electrochemical polymerization of PANI within the pores of the MOF. The presence of a conductive polymer within the pores of the MOF, greatly reduced the material's bulk electrical resistance while maintaining the MOF's high capacitance and rate of performance. The combination of the chemical properties of a conductive polymer and the physical properties of a MOF yield a supercapacitor (SC) that surpasses the performance of most of the other technologies currently available.[210]

PolyMOFs

The third category of MOF-polymer composite is called a polyMOF. This category can be defined as the controlled and ordered integration of one-dimensional, non-porous, amorphous polymers into metal–organic frameworks through a cross-linking reaction of the organic linker secondary building units (SBUs). This aspect of the SBU being directly integrated into the polymer makes polyMOFs unique from all other MOF-polymer composite materials. This cross-linking allows for the reversible conversion between standard MOFs and their composite polyMOF structures.[206, 211-213] This field saw its first major development when Cohen and coworkers chemically cross-linked 2-amino-1,4-benzene dicarboxylic acid (NH_2-BDC) within an IRMOF-3 structure.[213] This method has since been successfully demonstrated in many other MOF examples. Another example was in the use of cyclic diene metathesis polymerization to crosslink UiO-66.[212] One example of this new class of MOF composites that shows tremendous promise in advanced applications was demonstrated by Cohen and coworkers. In their work, Cohen and coworkers utilized the hydrophobicity of a polymer to stabilize IRMOF-1. As a single component, IRMOF-1 displays great selectivity toward CO_2 but also displays poor water stability. [214]

The potential applications for MOF-polymer composites include gas storage/separations,[215, 216] bio-imaging,[209] conductive materials,[210, 217] and even materials as electrodes in DSSCs.[218] With the range of potential applications ever growing for MOF-polymer composites, new synthetic techniques are needed to obtain novel structures and combinations that could yield new functionalities. One of the most promising techniques developed in recent years is the Sol-Gel processing of MOFs. Sol-gel processing can be used to chemically functionalize MOFs with moieties that can be used to generate unique polyMOFs, encapsulate MOFs and polymers generating core-shell composites, and evenly deposit MOF's into meso-/macroscale structures. These chemically functionalized MOFs can then be further hybridized with a large variety of materials.[219] For example, Taylor and coworkers generated a MOF@polymer core shell composite of

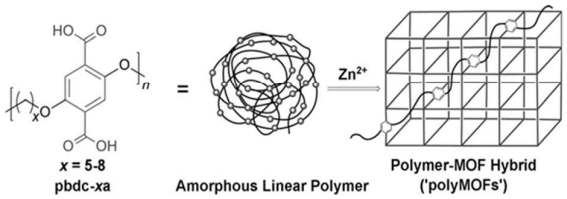

$Mn_3(BTC)_2$ coated with Polyvinylpyrrolidone (PVP) using a sol-gel processing technique. The unique properties of the resulting composites allowed them to be successfully tested as a material for Magnetic Resonance Imaging (MRI) applications.[220]

Fig. 22 Illustration of the formation and structure of polyMOFs. Reprinted with permission from reference 203. Copyright © 2015 WILEY-VCH Verlag GmbH and Co. KGaA, Weinheim.

MOF-nanoparticle composites

The earliest investigations of MOF-NP composites were generally restricted to NPs primarily being grown on the surface of MOF crystals or vice versa. These studied yielded great results, but they also had their fair share of limitations. The limitations included a lack of control over NP size, shape, and aggregation. Another limitation was that the required synthetic conditions were not always suited to all the components that formed the composite. However, it was hypothesized that the encapsulation or growth of a NPs "within" the pore of a MOF would solve most of the issues faced by earlier NP@MOF composites. This idea was based on the knowledge that MOFs have tenable sizes, chemical environments, and shapes. In later works, two distinct general methodologies were developed for the encapsulation of nanoparticles within the pores of a MOF. The first and most widely used methodologies is referred to as the "ship in a bottle'' method. This method can be described as the growing of a NP within the pores of a pre-formed MOF. Some of the techniques that fall under this process include the solution infiltration technique, chemical vapor deposition, solid grinding technique, and dual solvent technique. The second general method is called the "bottle around the ship'' or templated synthesis approach. This method can be summarized by first growing the intended nanoparticles followed by the growth of the desired MOF around the NPs. With these concepts in mind, MOF-nanoparticle composites can be further classified into 5 classes based on their non-MOF components: (a) Metal Nanoparticles (MNPs)(i.e. Au or Pd), (b) Oxide Based Nanoparticles (i.e. Fe_3O_4, GrO), (c) Non-Metal Based Nanoparticles (i.e. Carbon Nanotubes, Silica), (d) Quantum Dots (QDs), and (e) Polyoxometalates (POMs).[131, 193, 195, 200, 201, 203, 221-228]

MOF-Metal Nanoparticles Composites

The first subclass, MOF-metal nanoparticle composites, provides a great platform for various applications especially in the development of new catalysts.[221, 222, 226, 229] For example, it has been known that the catalytic activity of NP's generally

decreases with a decrease in reactive surface area.[230] The encapsulation of NP within a MOF's pores however allows for the NPs size and shape to be controlled. This in turn controls the reactive surface area of the NP. Various MNP@MIL-101 composites have been synthesized and the results validated that decreasing the size of the nanoparticle, increases the surface area of the NP, yielding a more effective and efficient catalyst. An example of the impact of the use of nanoparticle MOF composites is in the study by Xu and coworkers. In their study of catalytic efficiency using AuNi@MIL-101, it was found that the production of the desired ammonia borane was significantly increased with a decrease in NP size encapsulated in the MOF.[231]

Other pioneering work for generating advanced and functional catalysts using MOF-NP composites was performed by the Yaghi group. From their work, it was found that encapsulated NP's perform very differently in terms of substrate and product selectivity depending on the location of the NP on the interior or exterior of the MOF pore. By generating Pt@UiO-66 instead of Pt-*on*-UiO-66, where @ indicates that the nanoparticle is within the pores of the MOF, an extremely unique reaction pathway for the generation of benzene from methyl-cyclopropane (MCP) was obtained. This extremely rare product distribution can be further increased by approximately 9% by changing the parent MOF to UiO-67. Furthermore, changing the parent MOF from UiO-66 to UiO-67 also increases the catalyst Turn Over Frequency (TOF) by 31%. However, using MOF-801 completely eliminated benzene as an obtainable product. The Yaghi group also demonstrated that changing the chemical environment of the MOF, by changing the functionality of the organic linker SBU used, has a major effect on the catalyst selectivity, yield, and TOF.[232, 233] MNP@MOF's have also shown success in other catalytic pathways such as the oxidation of hydrocarbons, hydrogenation reactions,[234-237] and carbon-carbon cross coupling reactions.[238-242] For example, Pt@PCN-224 was the first report ever to use a MOF for the photo-oxidation of aromatic alcohols.[243]

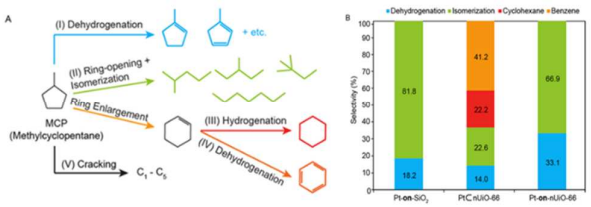

Fig. 23 (A) Schematic reaction diagram of hydrogenative conversion of MCP. (B) Product selectivity obtained at 150 °C over three catalysts (Pt-on-SiO2, Pt⊂nUiO-66, and Pt-on-nUiO-66). Reprinted with permission from reference 228. Copyright © 2014, American Chemical Society.

The formation of a MNP-MOF composite has also resulted in the improvement of hydrogen production,[244, 245] hydrogen storage,[246] separation of noble gases,[247] and sensing applications.[248, 249] For example, Au@MIL-101 was demonstrated to be a novel material for highly sensitive Surface-Enhanced Raman Scattering (SERS) applications. The large surface areas of the Au nanoparticles contained within the Au@MIL-101 allowed for preferential adsorption of an analyte close to the SERS-active sites. Overall, this dramatically enhanced the peak intensities and signal to noise ratio seen in the resultant spectrum. Au@MIL-101 was proven to be specifically successful for the detection of the organic pollutant *p*-phenylenediamine, and was also useful as a tumor marker for alpha-fetoprotein.[248] In another study, Tang and coworkers reported a novel "sandwich" type composite that had the ability to selectively tune catalysis as shown in Figure 24. The "sandwich" structure allowed for the catalytic performance of the composite to be tuned away from the highly favorable hydrogenation of the carbon–carbon bonds, to the much less favorably selective hydrogenation of the carbon–oxygen bonds. With this new catalytic pathway easily accessible, MIL-101@Pt@MIL-101 was successfully tested as a catalyst for the selective reduction of α,β-unsaturated aldehydes to unsaturated alcohols.[237]

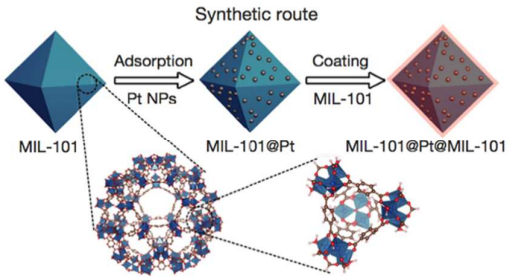

Fig. 24 Synthetic route to generate sandwich MIL-101@Pt@MIL-101. Reprinted with permission from reference 233. Copyright © 2016, Rights Managed by Nature Publishing Group

.

MOF-Metal Oxide Composites

The next class of NP-MOF composites contain oxide-based NPs. This class of materials has properties that vary based on the synthetic method used to generate the material. For example, four different derivatives of Fe_3O_4@MIL-101 can be made simply by changing the methods used in synthesis. The four methods used in this particular study were "ship in a bottle", direct sonication mixing, "bottle around a ship", and heterogeneous co-precipitation. The "ship in a bottle'' method resulted in excellent performance in the oxidation of different substituted benzyl alcohols forming benzaldehydes.[250] The direct mixing approach used sonication and produced a composite that could be used to perform solid-phase extractions of polycyclic aromatic hydrocarbons.[251] The "bottle around a ship" method produced a composite that showed great promise in a variety of gas storage applications.[252] Lastly, the "heterogeneous co-precipitation" method did not require the pre-synthesis modification of the magnetic Fe_3O_4 nanoparticles. This method yielded a sample of Fe_3O_4@MIL-

101 that exhibited BET surfaces areas and pore volumes that had not previously been achieved with MIL-101. The other major benefit of this method is that the encapsulated NPs retain their unique magnetic properties. Li and coworkers demonstrated that the "heterogeneous co-precipitation" method significantly increased the performance of MIL-101 as a material for advanced separations, such as the removal of toxic dyes from water.[253] Continuing this work in another study, it demonstrated that by changing the MOF in the backbone of the composite from MIL-100 to MIL-101, micro-solid-phase extraction of dopamine, epinephrine, and norepinephrine from biological samples was possible.[254]

Numerous metal-oxide based NP-MOF composites have also been reported as significantly improved catalysts when compared to traditional catalysts. One example was reported by Fisher and coworkers and was used for the oxidation of benzyl alcohols to benzaldehydes. This was successfully accomplished in a series of composites that contained MOF-5 as the backbone and nanoparticles such as ZnO, TiO_2, Au/ZnO, and Au/TiO_2. Other examples of NP-MOFs used in catalysis include CuO/CeO_2 encapsulated nanoparticles in HKUST-1 for carbon monoxide to carbon dioxide conversion,[255] graphene-oxide (GrO) based composites for adsorption of CO_2,[256] H_2,[257] NO2,[258] acetone,[259] *n*-hexane,[260] rhodamine-B,[261] and methylene blue,[262] composites for improved Li-S battery performance.[263] An additional enhanced adsorption capacity NP-MOF is graphite oxide based (GO)@MIL-101 which has been used for adsorption of sulfur-containing compounds (SCCs) and nitrogen-containing compounds (NCCs). Currently, (GO)@MIL-101 holds the record for highest adsorption capacity for nitrogen-containing compounds (NCCs) for any adsorbent material yet reported.[264]

MOF-Non-Metal Nanoparticle Composites

The third class of NP-MOF composites are generated when non-metal-based nanoparticles are hybridized with MOFs. A large quantity of the materials in this category are carbon nanotube (CNT) based. One such example is multi-walled carbon nanotube MIL-101 (MWCNT@MIL-101) and single-walled carbon nanotube MIL-101 (SWCNT@MIL-101). In this initial study it was found that the MWCNT composite demonstrated enhanced CO_2 capture[265] while the SWCNT composite had enhanced capacity for hydrogen storage. In another study with the same composites, Jasra and coworkers reported that SWCNT@MIL-101 displayed a 33% increase in gravimetric uptake capacity of H_2 over that of unadulterated MIL-101 at 77K and 60 bar.[266] Other studies with CNT incorporated composites include Li-doped CNT@HKUST-1 which was used to increase CH_4 adsorption,[267] and SWCNT@MIL-68 which was used for adsorption of phenols in aqueous solution.[268]

Other types of non-metal NP-MOFs that have successfully been hybridized are Si based nanoparticles,[227] graphene,[269] activated carbon,[270, 271] and carbon-nitrides.[272] An example of Si based nanoparticle composites was published by Wang and coworkers. In their work, they demonstrated that Si@ZIF-8 composites could be used as alternatives for high energy anode materials in lithium-ion batteries.[273] Another example of nonmetal NP-MOFs was published by Zhang and coworkers. In their work, they generated sphere-on-sphere (SOS)silica@HKUST-1 microspheres as the stationary phase in a chromatography column. It should be noted that although HKUST-1 is not a viable candidate for the separation of xylene isomers, the authors reported that their SOS@HKUST-1 composite achieved separation of the xylene isomers in under 5 minutes using the microsphere packed column. SOS@HKUST-1 packed columns have also proved successful in the separation of toluene/ethylbenzene/styrene and toluene/*o*-xylene/thiophene in under 1.5 min.[274]

MOF-Quantum Dots Composites

The fourth class of NP-MOF composites are generated when quantum dots (QDs) are encapsulated inside the pores of a MOF. To be effectively incorporated, nanocrystals must be less than 10 nm in size.[230] Current quantum dots that have been successfully made into QD@MOF composites include CdS, ZnS, CdSe, CdTe, and GaN. There is a vast range of potential uses for QD@MOFs, but currently, this type of composite has only really been tested for applications in molecular sensing, hydrogen production, light harvesting, and water splitting.[228] An example of a QD@MOF is in ZIF-8, with $CdSe_xS_{1-x}$/ZnS quantum dots encapsulated within the pores of the MOF. The resulting composite was stable and tested as an efficient white Light Emitting Diode (LED).[275]

Carbon-quantum dots (C-QDs), a subclass of quantum dots containing only carbon atoms, have also been incorporated into MOFs to generate C-QD@MOF composites. In a study similar to that of Peng and coworkers, C-QDs were encapsulated within ZIF-8. The results of their study indicated that the C-QD@ZIF-8 could be used as an ultrasensitive and highly selective composite for Cu^{2+} ion detection. This particular composite displayed a wide detection range (2 to 1000 nM) and a very low detection limit (80 pM).[276] In addition to these two studies, C-DQ@MOFs have also been used as pH sensitive anticancer drug delivery platforms.[277]

MOF-Polyoxometalates Composites

The final class of NP-MOF composites contain polyoxometalates (POMs). MOFs provide a platform for the stabilization of POMs without reducing the wide range of magnetic, redox active, and catalytic properties traditionally associated with POMs. Polyoxometalates have been encapsulated in a variety of MOF systems such as UiO-67,[278] MIL-101, and MIL-100.[279] As seen through the investigation of POM@MIL-101(Cr), changing the identity of the POM significantly changes the composite properties and applications. POM@MOFs have been generated using Zn, Fe, Cr, and Co functionalized POMs and have resulted in applications that range from electro-catalysis to desulfurization of gasoline. A famous example of POM@MOFs is that of PW_{11}@MIL-101 and SiW_{11}@MIL-101 which show promise as liquid phase oxidation catalysts.[280, 281]

MOF-enzyme composites

Enzymes are defined as naturally occurring biological catalysts, and are known to display properties of high reactivity, selectivity, yield and specificity. Unlike most traditional catalysts, enzymatic catalysts are most effective at very mild conditions. Unfortunately, enzyme catalytic transformations have not been successfully scaled to the industrial level due to their low operational stability, difficulty of recovery, narrow optimum pH ranges, and substantial loss of enzyme activity over time. There have been many attempts to solve these problems in the industrial scale. These strategies have mainly been focused on immobilization of enzymes on solid supports including sol–gel matrices, hydrogels, organic micro-particles, and mesoporous silica composites. However, many of the materials used in the immobilization approach lack sufficient adsorbate-adsorbent interactions. This ultimately leads to enzyme leaching which significantly reduces the lifetime of the catalyst, preventing these composites from be used on the industrial scale.[202, 282, 283]

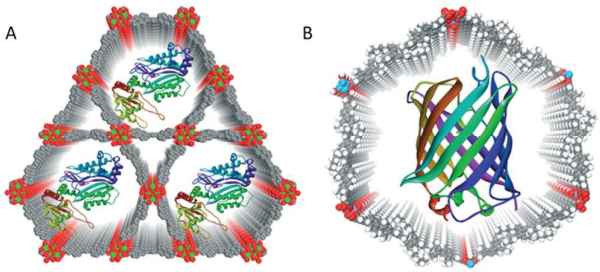

Fig. 25 A) Representation of encapsulation of organophosphorus acid anhydrolase (OPAA) in the hierarchical channel-type Zr-MOF, NU- 1003. B) Encapsulation of GFP in IRMOF-74-IX. Reprinted with permission from reference 279. Copyright © 2007 Journal of the American Chemical Society.

In light of the issues previously associated with enzyme immobilization, there has been significant interest in using MOFs as a new platform for the immobilization of enzymes as MOFs may be able to provide additional stability without a negative impact on enzyme activity. To date, the various methods that have been employed to generate MOF-enzyme composites are: surface attachment, covalent linkage, co-precipitation, and pore encapsulation.[202]

Surface attachment is defined as a method that utilizes the weak MOF-enzyme interactions in order to attach enzymes onto the surface of the MOF particles. Some examples of composites generated using the surface attachment method are GOx-*on*-MIL-100(Fe), Lipase-*on*-HKUST-1, and Trypsin-*on*-CYCU-4. These composites have been used in applications such as the electrolytic detection of glucose, catalysis of esterification reactions, and Warfarin synthesis.[284-286]

In the covalent linkage method, the free amino groups of the enzymes form one or more peptide bonds with the carboxylate groups on the MOF surface. Various MOF-enzyme composites generated using this method are Hermin@MIL-101-NH_2(Al), GFP/Lipase@IRMOF-3, and SEH@UiO-66-NH_2. These composites have been applied to glucose detection, catalysis of transesterification, and asymmetric hydrolysis reactions.[285-287]

Co-precipitation has also been used to generate a wide variety of ZIF-8 based composites with enzymes such as lipase, GoX, HRP, and Cyt-C. The theme of these ZIF-enzyme composites is that they all show enhanced tolerance to molecules such as trypsin, proteinase K, EDTA, and various organic solvents; all of which are known to denature enzymes.[168, 288-290]

The final method mentioned here is the method of pore encapsulation. Pore encapsulation has been identified as one of the most promising techniques that could solve the issues associated with other enzyme-composite materials. The two reasons for the success of pore encapsulation is that MOFs can be successfully synthesized with many different functionalities and pore environments as well as a vast range of pore sizes. In the initial stages of MOF development, the pore sizes were simply too small to successfully encapsulate enzymes. However, as described in sections 2.1 and 5.2, generating mesoporous and hierarchically porous MOFs has been more successful in recent years. While the microporous range is generally not suitable for the encapsulation of most enzymes due their relatively large size, MOFs with mesoporous cavities represent a remarkable class of materials for the encapsulation of enzymes immobilization applications for 3 main reasons: (a) Mesopores cavities yield high enzyme loading due to enhanced pore volume and void spaces, (b) Enzymes can be physically adsorbed into the cavity instead of dangling on the MOF surface leading to improved stability and reduced leaching in recycled usage, and (c) Mesopores can provide size selectivity for specific substrates, which can rarely be achieved with surface immobilized enzymes.[202]

One of the first examples of enzyme encapsulation in mesoporous cavities was published by Ma and coworkers in 2011. This report utilized a terbium based mesoporous MOF (Tb-mesoMOF) that possessed a hierarchical porous structure with diameters of 0.9, 3.0 and 4.1 nm for the encapsulation of Microperoxidase-11 (MP-11). When compared to free MP-11 and MP-11@MCM-41, a silica based composite, MP-11@Tb-mesoMOF displayed the highest conversion rate and high reaction rate when used in the oxidation reaction of 3,5-di-tert-butyl-catechol. MP-11@Tb-mesoMOF also did not produce any unwanted side products due to the prevention of enzyme aggregation.[291]

Zhou and coworkers have also made major contributions to this field. PCN-333(Al) demonstrated an extremely high enzyme loading capacity for HRP, Cyt-C, and MP-11 due to favorable interactions between the pore surface and the enzyme. Once immobilized within the pore of the MOF structure, the enzymes demonstrate lower K_m values than free enzymes, suggesting that immobilized enzymes require a lower substrate concentration to achieve the maximum conversion rate. Lower K_m values also indicate that the enzyme@PCN-333(Al) variants have a higher substrate selectivity than the free enzyme counterparts.[292]

As successful enzyme incorporation is tied to pore size distributions, the enlargement of pores in a MOF through isoreticular expansion has been a highly useful technique. Isoreticular expansion has been applied to a wide range of enzyme@MOF composites. For example, PCN-333 can be isoreticularly expanded to generate PCN-888. Pores as large as 6.2nm can be generated for PCN-888 using this method. In a study by Zhou and coworkers, the authors were able to utilize the large pores of PCN-888 to simultaneously immobilize two enzymes (GOx and HRP), yielding a tandem enzymatic nanoreactor. The nanoreactor displayed excellent catalytic performances and negligible enzyme leaching over several cycles. The composite also displayed stability toward trypsin digestion suggesting this nanoreactor could be used in various *in vivo* and *in vitro* applications.[293]

A third example published in 2017 by Zhou and coworkers reported Cyt-C@CYCU-3. This composite was successful for the oxidation of ABTS and *o*-PDA. In addition, when linker labilization was used to generate a hierarchically porous (HP) structure, a significant increase in the composite performance was obtained. Cyt-C@HP-CYCU-3 displayed catalytic activity similar to the free enzyme due to an increased void space leading to enhanced substrate diffusion to the enzymes active site.[161] Hupp and coworkers validated these findings when they demonstrated the critical role of the hierarchical structure of NU-1000 for enzyme encapsulation applications.[294]

The recent work of the Ma, Zhou, Hupp, and other research groups have shown that the formation of enzyme-MOF composites, especially enzymes encapsulated within the pores of a MOF, has resulted in one of the leading candidates for enzyme immobilization.

Summary and Outlook

MOFs have proven to be one of the most versatile materials that are available for research and applications in today's modern world. These unique structures have offered an ever-expanding knowledge basis for a wide range of uses. In this review, the a small portion of the recent advances in the study of Metal-Organic Frameworks has been discussed. Studies on the optimized design, functionalization, and stabilization of MOFs have been a fundamental basis of discovery in the past. Based on the knowledge gained from isoreticular expansion techniques, topology-guided designs, modulated syntheses, and post-synthetic modification strategies, researchers have been able to expand the MOF family with sophisticated, highly tuned, rationally designed structures.

Stability and the nature of metal ligand bonding has been at the heart of MOF chemistry for a considerable amount of time. A traditionally long-standing problem for MOF chemistry, new research into increased MOF stability has been able to overcome by many issues that faced early MOF structures. The most commonly used strategies for increasing MOF stability today are the utilization of high-valent metal-carboxylate frameworks or low-valent metal azolate frameworks as they have been shown to enhance both the chemical and thermal stability of MOFs. Indeed, many challenges still exist regarding MOF stability, as the most stable MOFs are still not comparable with other porous materials including zeolites, mesoporous silica, and porous carbons. However, the high tunability and diversity of available MOF structures indicate that future improvements for MOF stability is certainly achievable.

In recent years, MTV-MOFs with multiple functionalities have arisen as a uniquely integrated functional system. These composite systems have shown exciting potential in applications for gas adsorption, separation, and cooperative catalysis. Studies have shown that MTV-MOF systems exhibit improved performance, compared to the sum of the individual parts, towards desired applications.

In this review, we have also covered a small fraction of the emerging topics in MOFs regarding defect prevention and incorporation within MOF structures. Additionally, the newly emerging classifications of MOF composites have also been covered, with the predominate groups outlined within being polymers, nanoparticles, and enzymes.

These cutting-edge directions combine the interests of a variety of fields such as MOF chemistry, polymer chemistry, nano-chemistry, physics, computational studies, and biology. The unique cross roads of disciplines found within the study of MOFs has helped to promote the further development of MOFs as an interdisciplinary study.

Conflicts of interest

There are no conflicts to declare.

Acknowledgements

The authors of this review were each supported in part by the Center for Gas Separations Relevant to Clean Energy Technologies, an Energy Frontier Research Center funded by the U.S. Department of Energy, Office of Science, Basic Energy Sciences under Award Number DE-SC0001015, the Robert A. Welch Foundation through a Welch Endowed Chair to HJZ (A-0030), the U.S. Department of Energy Office of Fossil Energy, National Energy Technology Laboratory (DE-FE0026472), the National Science Foundation under Grant No. 1632486, and by the Qatar National Research Fund under Award Number NPRP9-377-1-080.

References

1. O. M. Yaghi, G. Li and H. Li, *Nature (London)*, 1995, **378**, 703-706.
2. H. Li, M. Eddaoudi, T. L. Groy and O. M. Yaghi, *J. Am. Chem. Soc.*, 1998, **120**, 8571-8572.
3. M. Kondo, T. Yoshitomi, K. Seki, H. Matsuzaka and S. Kitagawa, *Angew. Chem., Int. Ed. Engl.*, 1997, **36**, 1725-1727.

4. B. C. Hughes, C. R. Murdock and D. M. Jenkins, *Inorg. Chem. Front.*, 2015, **2**, 1001-1005.
5. M. T. Wharmby, J. P. S. Mowat, S. P. Thompson and P. A. Wright, *J. Am. Chem. Soc.*, 2011, **133**, 1266-1269.
6. O. Delgado Friedrichs, M. O'Keeffe and O. M. Yaghi, *Solid State Sci.*, 2003, **5**, 73-78.
7. M. Eddaoudi, J. Kim, N. Rosi, D. Vodak, J. Wachter, M. O'Keeffe and O. M. Yaghi, *Science (Washington, DC, U. S.)*, 2002, **295**, 469-472.
8. H. Furukawa, Y. B. Go, N. Ko, Y. K. Park, F. J. Uribe-Romo, J. Kim, M. O'Keeffe and O. M. Yaghi, *Inorg. Chem.*, 2011, **50**, 9147-9152.
9. O. M. Yaghi, M. O'Keeffe, N. W. Ockwig, H. K. Chae, M. Eddaoudi and J. Kim, *Nature (London, U. K.)*, 2003, **423**, 705-714.
10. Y. Bai, Y. Dou, L.-H. Xie, W. Rutledge, J.-R. Li and H.-C. Zhou, *Chem. Soc. Rev.*, 2016, **45**, 2327-2367.
11. K. Sumida, D. L. Rogow, J. A. Mason, T. M. McDonald, E. D. Bloch, Z. R. Herm, T.-H. Bae and J. R. Long, *Chem. Rev. (Washington, DC, U. S.)*, 2012, **112**, 724-781.
12. J. Y. Lee, O. K. Farha, J. Roberts, K. A. Scheidt, S. B. T. Nguyen and J. T. Hupp, *Chem. Soc. Rev.*, 2009, **38**, 1450-1459.
13. S. Ma and H.-C. Zhou, *Chem. Commun. (Cambridge, U. K.)*, 2010, **46**, 44-53.
14. M. Yoon, R. Srirambalaji and K. Kim, *Chem. Rev. (Washington, DC, U. S.)*, 2012, **112**, 1196-1231.
15. C. Orellana-Tavra, E. F. Baxter, T. Tian, T. D. Bennett, N. K. H. Slater, A. K. Cheetham and D. Fairen-Jimenez, *Chem. Commun. (Cambridge, U. K.)*, 2015, **51**, 13878-13881.
16. J. Della Rocca, D. Liu and W. Lin, *Acc. Chem. Res.*, 2011, **44**, 957-968.
17. P. Horcajada, R. Gref, T. Baati, P. K. Allan, G. Maurin, P. Couvreur, G. Ferey, R. E. Morris and C. Serre, *Chem. Rev. (Washington, DC, U. S.)*, 2012, **112**, 1232-1268.
18. P. Horcajada, C. Serre, G. Maurin, N. A. Ramsahye, F. Balas, M. Vallet-Regi, M. Sebban, F. Taulelle and G. Ferey, *J. Am. Chem. Soc.*, 2008, **130**, 6774-6780.
19. A. C. McKinlay, R. E. Morris, P. Horcajada, G. Ferey, R. Gref, P. Couvreur and C. Serre, *Angew. Chem., Int. Ed.*, 2010, **49**, 6260-6266.
20. E. R. Parnham and R. E. Morris, *Acc. Chem. Res.*, 2007, **40**, 1005-1013.
21. D.-K. Bucar, G. S. Papaefstathiou, T. D. Hamilton, Q. L. Chu, I. G. Georgiev and L. R. MacGillivray, *Eur. J. Inorg. Chem.*, 2007, DOI: 10.1002/ejic.200700442, 4559-4568.
22. A. K. Cheetham, G. Ferey and T. Loiseau, *Angew. Chem., Int. Ed.*, 1999, **38**, 3268-3292.
23. M. Dinca, A. Dailly and J. R. Long, *Chem. - Eur. J.*, 2008, **14**, 10280-10285.
24. M. Dinca and J. R. Long, *Angew. Chem., Int. Ed.*, 2008, **47**, 6766-6779.
25. S. S. Y. Chui, S. M. F. Lo, J. P. H. Charmant, A. G. Orpen and I. D. Williams, *Science (Washington, D. C.)*, 1999, **283**, 1148-1150.
26. J. Lu, A. Mondal, B. Moulton and M. J. Zaworotko, *Angew. Chem., Int. Ed.*, 2001, **40**, 2113-2116.
27. L. Xie, S. Liu, C. Gao, R. Cao, J. Cao, C. Sun and Z. Su, *Inorg. Chem.*, 2007, **46**, 7782-7788.
28. M. Kramer, U. Schwarz and S. Kaskel, *J. Mater. Chem.*, 2006, **16**, 2245-2248.
29. L. J. Murray, M. Dinca, J. Yano, S. Chavan, S. Bordiga, C. M. Brown and J. R. Long, *J. Am. Chem. Soc.*, 2010, **132**, 7856-7857.
30. J. B. DeCoste, G. W. Peterson, H. Jasuja, T. G. Glover, Y.-g. Huang and K. S. Walton, *J. Mater. Chem. A*, 2013, **1**, 5642-5650.
31. S. Biswas, T. Ahnfeldt and N. Stock, *Inorg. Chem.*, 2011, **50**, 9518-9526.
32. S. Biswas, D. E. P. Vanpoucke, T. Verstraelen, M. Vandichel, S. Couck, K. Leus, Y.-Y. Liu, M. Waroquier, V. Van Speybroeck, J. F. M. Denayer and P. Van Der Voort, *J. Phys. Chem. C*, 2013, **117**, 22784-22796.
33. S. Couck, J. F. M. Denayer, G. V. Baron, T. Remy, J. Gascon and F. Kapteijn, *J. Am. Chem. Soc.*, 2009, **131**, 6326-6327.
34. S. Surble, C. Serre, C. Mellot-Draznieks, F. Millange and G. Ferey, *Chem. Commun. (Cambridge, U. K.)*, 2006, DOI: 10.1039/B512169H, 284-286.
35. T. C. Wang, W. Bury, D. A. Gomez-Gualdron, N. A. Vermeulen, J. E. Mondloch, P. Deria, K. Zhang, P. Z. Moghadam, A. A. Sarjeant, R. Q. Snurr, J. F. Stoddart, J. T. Hupp and O. K. Farha, *J. Am. Chem. Soc.*, 2015, **137**, 3585-3591.
36. Y.-S. Bae, A. O. Yazaydin and R. Q. Snurr, *Langmuir*, 2010, **26**, 5475-5483.
37. M. Li, D. Li, M. O'Keeffe and O. M. Yaghi, *Chem. Rev.* , 2014, **114**, 1343-1370.
38. D. Kim, X. Liu and M. S. Lah, *Inorg. Chem. Front.*, 2015, **2**, 336-360.
39. V. A. Blatov, L. Carlucci, G. Ciani and D. M. Proserpio, *CrystEngComm*, 2004, **6**, 377-395.

40. M. O'Keeffe and O. M. Yaghi, *Chem. Rev. (Washington, DC, U. S.)*, 2012, **112**, 675-702.
41. S. Ma, D. Sun, M. Ambrogio, J. A. Fillinger, S. Parkin and H.-C. Zhou, *J. Am. Chem. Soc.*, 2007, **129**, 1858-1859.
42. J. Zhang, L. Wojtas, R. W. Larsen, M. Eddaoudi and M. J. Zaworotko, *J Am Chem Soc*, 2009, **131**, 17040-17041.
43. B. Chen, X. Wang, Q. Zhang, X. Xi, J. Cai, H. Qi, S. Shi, J. Wang, D. Yuan and M. Fang, *J. Mater. Chem.*, 2010, **20**, 3758-3767.
44. O. Shekhah, H. Wang, M. Paradinas, C. Ocal, B. Schuepbach, A. Terfort, D. Zacher, R. A. Fischer and C. Woell, *Nat. Mater.*, 2009, **8**, 481-484.
45. D. A. Gomez-Gualdron, O. V. Gutov, V. Krungleviciute, B. Borah, J. E. Mondloch, J. T. Hupp, T. Yildirim, O. K. Farha and R. Q. Snurr, *Chem. Mater.*, 2014, **26**, 5632-5639.
46. O. V. Gutov, W. Bury, D. A. Gomez-Gualdron, V. Krungleviciute, D. Fairen-Jimenez, J. E. Mondloch, A. A. Sarjeant, S. S. Al-Juaid, R. Q. Snurr, J. T. Hupp, T. Yildirim and O. K. Farha, *Chem. - Eur. J.*, 2014, **20**, 12389-12393.
47. T.-F. Liu, D. Feng, Y.-P. Chen, L. Zou, M. Bosch, S. Yuan, Z. Wei, S. Fordham, K. Wang and H.-C. Zhou, *J. Am. Chem. Soc.*, 2015, **137**, 413-419.
48. H. Chun, D. Kim, D. N. Dybtsev and K. Kim, *Angew. Chem., Int. Ed.*, 2004, **43**, 971-974.
49. J. M. Gotthardt, K. F. White, B. F. Abrahams, C. Ritchie and C. Boskovic, *Cryst. Growth Des.*, 2012, **12**, 4425-4430.
50. O. Delgado-Friedrichs, M. O'Keeffe and O. M. Yaghi, *Phys. Chem. Chem. Phys.*, 2007, **9**, 1035-1043.
51. M. Zhang, Y.-P. Chen, M. Bosch, T. Gentle, III, K. Wang, D. Feng, Z. U. Wang and H.-C. Zhou, *Angew. Chem., Int. Ed.*, 2014, **53**, 815-818.
52. S. Yuan, W. Lu, Y.-P. Chen, Q. Zhang, T.-F. Liu, D. Feng, X. Wang, J. Qin and H.-C. Zhou, *J. Am. Chem. Soc.*, 2015, **137**, 3177-3180.
53. T. Tsuruoka, S. Furukawa, Y. Takashima, K. Yoshida, S. Isoda and S. Kitagawa, *Angew. Chem., Int. Ed.*, 2009, **48**, 4739-4743, S4739/4731-S4739/4738.
54. S. Diring, S. Furukawa, Y. Takashima, T. Tsuruoka and S. Kitagawa, *Chemistry of Materials*, 2010, **22**, 4531-4538.
55. A. Umemura, S. Diring, S. Furukawa, H. Uehara, T. Tsuruoka and S. Kitagawa, *J. Am. Chem. Soc.*, 2011, **133**, 15506-15513.
56. A. Schaate, P. Roy, A. Godt, J. Lippke, F. Waltz, M. Wiebcke and P. Behrens, *Chem. - Eur. J.*, 2011, **17**, 6643-6651, S6643/6641-S6643/6611.
57. G. Wissmann, A. Schaate, S. Lilienthal, I. Bremer, A. M. Schneider and P. Behrens, *Microporous Mesoporous Mater.*, 2012, **152**, 64-70.
58. F. Vermoortele, B. Bueken, G. Le Bars, B. Van de Voorde, M. Vandichel, K. Houthoofd, A. Vimont, M. Daturi, M. Waroquier, V. Van Speybroeck, C. Kirschhock and D. E. De Vos, *J. Am. Chem. Soc.*, 2013, **135**, 11465-11468.
59. S. Yuan, L. Feng, K. Wang, J. Pang, M. Bosch, C. Lollar, Y. Sun, J. Qin, X. Yang, P. Zhang, Q. Wang, L. Zou, Y. Zhang, L. Zhang, Y. Fang, J. Li and H.-C. Zhou, *Adv. Mater. (Weinheim, Ger.)*, 2018, DOI: 10.1002/adma.201704303, Ahead of Print.
60. A. Ferguson, L. Liu, S. J. Tapperwijn, D. Perl, F.-X. Coudert, S. Van Cleuvenbergen, T. Verbiest, M. A. van der Veen and S. G. Telfer, *Nat. Chem.*, 2016, **8**, 250-257.
61. G. C. Shearer, S. Chavan, S. Bordiga, S. Svelle, U. Olsbye and K. P. Lillerud, *Chem. Mater.*, 2016, **28**, 3749-3761.
62. X. Lian, Y. Fang, E. Joseph, Q. Wang, J. Li, S. Banerjee, C. Lollar, X. Wang and H.-C. Zhou, *Chem. Soc. Rev.*, 2017, **46**, 3386-3401.
63. M. Kim and S. M. Cohen, *CrystEngComm*, 2012, **14**, 4096-4104.
64. Z. Saedi, V. Safarifard and A. Morsali, *Microporous Mesoporous Mater.*, 2016, **229**, 51-58.
65. S. J. Garibay, Z. Wang and S. M. Cohen, *Inorg. Chem.*, 2010, **49**, 8086-8091.
66. P. Roy, A. Schaate, P. Behrens and A. Godt, *Chem. - Eur. J.*, 2012, **18**, 6979-6985, S6979/6971-S6979/6915.
67. Y. Goto, H. Sato, S. Shinkai and K. Sada, *J. Am. Chem. Soc.*, 2008, **130**, 14354-14355.
68. T. Gadzikwa, O. K. Farha, C. D. Malliakas, M. G. Kanatzidis, J. T. Hupp and S. T. Nguyen, *J. Am. Chem. Soc.*, 2009, **131**, 13613-13615.
69. T. Gadzikwa, G. Lu, C. L. Stern, S. R. Wilson, J. T. Hupp and S. T. Nguyen, *Chem. Commun. (Cambridge, U. K.)*, 2008, DOI: 10.1039/b805101a, 5493-5495.
70. M. Savonnet, D. Bazer-Bachi, N. Bats, J. Perez-Pellitero, E. Jeanneau, V. Lecocq, C. Pinel and D. Farrusseng, *J. Am. Chem. Soc.*, 2010, **132**, 4518-4519.

71. R. J. Marshall and R. S. Forgan, *Eur. J. Inorg. Chem.*, 2016, **2016**, 4310-4331.
72. K. K. Tanabe and S. M. Cohen, *Chem. Soc. Rev.*, 2011, **40**, 498-519.
73. S. M. Cohen, *Chem. Rev. (Washington, DC, U. S.)*, 2012, **112**, 970-1000.
74. B. F. Hoskins and R. Robson, *J. Am. Chem. Soc.*, 1990, **112**, 1546-1554.
75. Y. H. Kiang, G. B. Gardner, S. Lee, Z. Xu and E. B. Lobkovsky, *J. Am. Chem. Soc.*, 1999, **121**, 8204-8215.
76. A. D. Burrows, C. G. Frost, M. F. Mahon and C. Richardson, *Chem. Commun. (Cambridge, U. K.)*, 2009, DOI: 10.1039/b906170c, 4218-4220.
77. A. D. Burrows, C. Frost, M. F. Mahon and C. Richardson, *Angew. Chem., Int. Ed.*, 2008, **47**, 8482-8486.
78. Y. H. Kiang, G. B. Gardner, S. Lee and Z. Xu, *J. Am. Chem. Soc.*, 2000, **122**, 6871-6883.
79. J. S. Seo, D. Whang, H. Lee, S. I. Jun, J. Oh, Y. J. Jeon and K. Kim, *Nature (London)*, 2000, **404**, 982-986.
80. Z. Wang and S. M. Cohen, *J. Am. Chem. Soc.*, 2007, **129**, 12368-12369.
81. H.-L. Jiang, D. Feng, T.-F. Liu, J.-R. Li and H.-C. Zhou, *J. Am. Chem. Soc.*, 2012, **134**, 14690-14693.
82. S. M. Cohen, *J. Am. Chem. Soc.*, 2017, **139**, 2855-2863.
83. L. Li, S. Tang, C. Wang, X. Lv, M. Jiang, H. Wu and X. Zhao, *Chem. Comm.*, 2014, **50**, 2304-2307.
84. M. I. Gonzalez, E. D. Bloch, J. A. Mason, S. J. Teat and J. R. Long, *Inorg. Chem.*, 2015, **54**, 2995-3005.
85. K.-K. Yee, N. Reimer, J. Liu, S.-Y. Cheng, S.-M. Yiu, J. Weber, N. Stock and Z. Xu, *J. Am. Chem. Soc.*, 2013, **135**, 7795-7798.
86. W. Morris, B. Volosskiy, S. Demir, F. Gandara, P. L. McGrier, H. Furukawa, D. Cascio, J. F. Stoddart and O. M. Yaghi, *Inorg. Chem.*, 2012, **51**, 6443-6445.
87. N. C. Thacker, Z. Lin, T. Zhang, J. C. Gilhula, C. W. Abney and W. Lin, *J. Am. Chem. Soc.*, 2016, **138**, 3501-3509.
88. X. Wang, W. Chen, L. Zhang, T. Yao, W. Liu, Y. Lin, H. Ju, J. Dong, L. Zheng, W. Yan, X. Zheng, Z. Li, X. Wang, J. Yang, D. He, Y. Wang, Z. Deng, Y. Wu and Y. Li, *J. Am. Chem. Soc.*, 2017, **139**, 9419-9422.
89. S. G. Dunning, G. Nandra, A. D. Conn, W. Chai, R. E. Sikma, J. S. Lee, P. Kunal, J. E. Reynolds, III, J.-S. Chang, A. Steiner, G. Henkelman and S. M. Humphrey, *Angew. Chem., Int. Ed.*, 2018, DOI: 10.1002/anie.201802402, Ahead of Print.
90. T. Yamada and H. Kitagawa, *J. Am. Chem. Soc.*, 2009, **131**, 6312-6313.
91. R. K. Deshpande, G. I. N. Waterhouse, G. B. Jameson and S. G. Telfer, *Chem. Commun. (Cambridge, U. K.)*, 2012, **48**, 1574-1576.
92. A. Sen Gupta, R. K. Deshpande, L. Liu, G. I. N. Waterhouse and S. G. Telfer, *CrystEngComm*, 2012, **14**, 5701-5704.
93. R. K. Deshpande, J. L. Minnaar and S. G. Telfer, *Angew. Chem., Int. Ed.*, 2010, **49**, 4598-4602, S4598/4591-S4598/4520.
94. D. J. Lun, G. I. N. Waterhouse and S. G. Telfer, *J. Am. Chem. Soc.*, 2011, **133**, 5806-5809.
95. M. J. Ingleson, R. Heck, J. A. Gould and M. J. Rosseinsky, *Inorg. Chem.*, 2009, **48**, 9986-9988.
96. J. G. Nguyen, K. K. Tanabe and S. M. Cohen, *CrystEngComm*, 2010, **12**, 2335-2338.
97. B. J. Burnett, P. M. Barron, C. Hu and W. Choe, *J. Am. Chem. Soc.*, 2011, **133**, 9984-9987.
98. M. Kim, J. F. Cahill, Y. Su, K. A. Prather and S. M. Cohen, *Chem. Sci.*, 2012, **3**, 126-130.
99. M. H. Beyzavi, N. A. Vermeulen, K. Zhang, M. So, C.-W. Kung, J. T. Hupp and O. K. Farha, *ChemPlusChem*, 2016, **81**, 708-713.
100. Y. Xu, N. A. Vermeulen, Y. Liu, J. T. Hupp and O. K. Farha, *Eur. J. Inorg. Chem.*, 2016, **2016**, 4345-4348.
101. T. Islamoglu, S. Goswami, Z. Li, A. J. Howarth, O. K. Farha and J. T. Hupp, *Acc. Chem. Res.*, 2017, **50**, 805-813.
102. O. Karagiaridi, W. Bury, J. E. Mondloch, J. T. Hupp and O. K. Farha, *Angew. Chem., Int. Ed.*, 2014, **53**, 4530-4540.
103. G. Gonzalez Miera, A. Bermejo Gomez, P. J. Chupas, B. Martin-Matute, K. W. Chapman and A. E. Platero-Prats, *Inorg. Chem.*, 2017, **56**, 4577-4584.
104. O. Karagiaridi, W. Bury, E. Tylianakis, A. A. Sarjeant, J. T. Hupp and O. K. Farha, *Chem. Mater.*, 2013, **25**, 3499-3503.
105. S. Bureekaew, S. Amirjalayer and R. Schmid, *J. Mater. Chem.*, 2012, **22**, 10249-10254.
106. W. Bury, D. Fairen-Jimenez, M. B. Lalonde, R. Q. Snurr, O. K. Farha and J. T. Hupp, *Chem. Mater.*, 2013, **25**, 739-744.

107. K. L. Mulfort, O. K. Farha, C. L. Stern, A. A. Sarjeant and J. T. Hupp, *J. Am. Chem. Soc.*, 2009, **131**, 3866-3868.
108. T. Li, M. T. Kozlowski, E. A. Doud, M. N. Blakely and N. L. Rosi, *J. Am. Chem. Soc.*, 2013, **135**, 11688-11691.
109. M. Lanchas, D. Vallejo-Sanchez, G. Beobide, O. Castillo, A. T. Aguayo, A. Luque and P. Roman, *Chem. Commun. (Cambridge, U. K.)*, 2012, **48**, 9930-9932.
110. H. Li, M. Eddaoudi, M. O'Keeffe and O. M. Yaghi, *Nature*, 1999, **402**, 276-279.
111. W. T. A. Harrison, R. W. Broach, R. A. Bedard, T. E. Gier, X. Bu and G. D. Stucky, *Chemistry of Materials*, 1996, **8**, 691-700.
112. W. Liang, R. Babarao, M. J. Murphy and D. M. D'Alessandro, *Dalton Transactions*, 2015, **44**, 1516-1519.
113. J. H. Cavka, S. Jakobsen, U. Olsbye, N. Guillou, C. Lamberti, S. Bordiga and K. P. Lillerud, *Journal of the American Chemical Society*, 2008, **130**, 13850-13851.
114. V. Guillerm, F. Ragon, M. Dan-Hardi, T. Devic, M. Vishnuvarthan, B. Campo, A. Vimont, G. Clet, Q. Yang, G. Maurin, G. Férey, A. Vittadini, S. Gross and C. Serre, *Angewandte Chemie International Edition*, 2012, **51**, 9267-9271.
115. G. Férey, C. Mellot-Draznieks, F. M. C. Serre1, S. S. J. Dutour1 and I. Margiolaki, *Science*, 2005, **309**, 2040-2042.
116. D. Feng, K. Wang, Z. Wei, Y.-P. Chen, C. M. Simon, R. K. Arvapally, R. L. Martin, M. Bosch, T.-F. Liu, S. Fordham, D. Yuan, M. A. Omary, M. Haranczyk, B. Smit and H.-C. Zhou, 2014, **5**, 5723.
117. B. Wang, A. P. Cote, H. Furukawa, M. O/'Keeffe and O. M. Yaghi, *Nature*, 2008, **453**, 207-211.
118. B. Chen, Z. Yang, Y. Zhu and Y. Xia, *Journal of Materials Chemistry A*, 2014, **2**, 16811-16831.
119. K. Wang, Xiu-Liang, D. Feng, J. Li, S. Chen, J. Sun, L. Song, Y. Xie, J.-R. Li and H.-C. Zhou, *J Am Chem Soc*, 2016, **138**, 914-919.
120. Xiu-Liang, K. Wang, B. Wang, J. Su, X. Zou, Y. Xie, J.-R. Li and H.-C. Zhou, *J Am Chem Soc*, 2016, **139**, 211-217.
121. H. X. Deng, C. J. Doonan, H. Furukawa, R. B. Ferreira, J. Towne, C. B. Knobler, B. Wang and O. M. Yaghi, *Science*, 2010, **327**, 846-850.
122. Y. J. Sun, L. X. Sun, D. W. Feng and H. C. Zhou, *Angew Chem Int Edit*, 2016, **55**, 6471-6475.
123. S. Yuan, J. S. Qin, L. F. Zou, Y. P. Chen, X. Wang, Q. Zhang and H. C. Zhou, *Journal of the American Chemical Society*, 2016, **138**, 6636-6642.
124. L. J. Liu, K. Konstas, M. R. Hill and S. G. Telfer, *Journal of the American Chemical Society*, 2013, **135**, 17731-17734.
125. S. Yuan, Y. P. Chen, J. S. Qin, W. G. Lu, L. F. Zou, Q. Zhang, X. Wang, X. Sun and H. C. Zhou, *J Am Chem Soc*, 2016, **138**, 8912-8919.
126. L. Feng, S. Yuan, L. L. Zhang, K. Tan, J. L. Li, A. Kirchon, L. M. Liu, P. Zhang, Y. Han, Y. J. Chabal and H. C. Zhou, *Journal of the American Chemical Society*, 2018, **140**, 2363-2372.
127. L. J. Wang, H. X. Deng, H. Furukawa, F. Gandara, K. E. Cordova, D. Peri and O. M. Yaghi, *Inorg Chem*, 2014, **53**, 5881-5883.
128. Q. Liu, H. J. Cong and H. X. Deng, *Journal of the American Chemical Society*, 2016, **138**, 13822-13825.
129. S. Yuan, Y. P. Chen, J. S. Qin, W. G. Lu, X. Wang, Q. Zhang, M. Bosch, T. F. Liu, X. Z. Lian and H. C. Zhou, *Angew Chem Int Edit*, 2015, **54**, 14696-14700.
130. H. C. Zhou, J. R. Long and O. M. Yaghi, *Chem Rev*, 2012, **112**, 673-674.
131. P. Silva, S. M. Vilela, J. P. Tome and F. A. Almeida Paz, *Chem Soc Rev*, 2015, **44**, 6774-6803.
132. J. R. Li, J. Sculley and H. C. Zhou, *Chem Rev*, 2012, **112**, 869-932.
133. H. Furukawa, U. Muller and O. M. Yaghi, *Angew Chem Int Ed Engl*, 2015, **54**, 3417-3430.
134. Z. Fang, B. Bueken, D. E. De Vos and R. A. Fischer, *Angew Chem Int Ed Engl*, 2015, **54**, 7234-7254.
135. D. S. Sholl and R. P. Lively, *J Phys Chem Lett*, 2015, **6**, 3437-3444.
136. M. Vandichel, J. Hajek, F. Vermoortele, M. Waroquier, D. E. De Vos and V. Van Speybroeck, *CrystEngComm*, 2015, **17**, 395-406.
137. J. Canivet, M. Vandichel and D. Farrusseng, *Dalton Trans*, 2016, **45**, 4090-4099.
138. T. D. Bennett, A. K. Cheetham, A. H. Fuchs and F. X. Coudert, *Nat Chem*, 2016, **9**, 11-16.
139. L. Valenzano, B. Civalleri, S. Chavan, S. Bordiga, M. H. Nilsen, S. Jakobsen, K. P. Lillerud and C. Lamberti, *Chemistry of Materials*, 2011, **23**, 1700-1718.

140. S. B. Kalidindi, S. Nayak, M. E. Briggs, S. Jansat, A. P. Katsoulidis, G. J. Miller, J. E. Warren, D. Antypov, F. Cora, B. Slater, M. R. Prestly, C. Marti-Gastaldo and M. J. Rosseinsky, *Angew Chem Int Ed Engl*, 2015, **54**, 221-226.
141. A. W. Thornton, R. Babarao, A. Jain, F. Trousselet and F. X. Coudert, *Dalton Trans*, 2016, **45**, 4352-4359.
142. Z. Hu, I. Castano, S. Wang, Y. Wang, Y. Peng, Y. Qian, C. Chi, X. Wang and D. Zhao, *Crystal Growth & Design*, 2016, **16**, 2295-2301.
143. L. Zhou, X. Zhang and Y. Chen, *Materials Letters*, 2017, **197**, 167-170.
144. C. Atzori, G. C. Shearer, L. Maschio, B. Civalleri, F. Bonino, C. Lamberti, S. Svelle, K. P. Lillerud and S. Bordiga, *The Journal of Physical Chemistry C*, 2017, **121**, 9312-9324.
145. H. Wu, Y. S. Chua, V. Krungleviciute, M. Tyagi, P. Chen, T. Yildirim and W. Zhou, *J Am Chem Soc*, 2013, **135**, 10525-10532.
146. G. C. Shearer, S. Chavan, S. Bordiga, S. Svelle, U. Olsbye and K. P. Lillerud, *Chemistry of Materials*, 2016, **28**, 3749-3761.
147. X. Sang, J. Zhang, J. Xiang, J. Cui, L. Zheng, J. Zhang, Z. Wu, Z. Li, G. Mo, Y. Xu, J. Song, C. Liu, X. Tan, T. Luo, B. Zhang and B. Han, *Nat Commun*, 2017, **8**, 175.
148. F. Vermoortele, R. Ameloot, L. Alaerts, R. Matthessen, B. Carlier, E. V. R. Fernandez, J. Gascon, F. Kapteijn and D. E. De Vos, *Journal of Materials Chemistry*, 2012, **22**.
149. G. Barin, V. Krungleviciute, O. Gutov, J. T. Hupp, T. Yildirim and O. K. Farha, *Inorg Chem*, 2014, **53**, 6914-6919.
150. S. M. Cohen, *Chem Rev*, 2012, **112**, 970-1000.
151. G. C. Shearer, S. Chavan, J. Ethiraj, J. G. Vitillo, S. Svelle, U. Olsbye, C. Lamberti, S. Bordiga and K. P. Lillerud, *Chemistry of Materials*, 2014, **26**, 4068-4071.
152. S. Gadipelli and Z. Guo, *Chemistry of Materials*, 2014, **26**, 6333-6338.
153. J. B. DeCoste, G. W. Peterson, B. J. Schindler, K. L. Killops, M. A. Browe and J. J. Mahle, *Journal of Materials Chemistry A*, 2013, **1**.
154. C. Montoro, P. Ocon, F. Zamora and J. A. Navarro, *Chemistry*, 2016, **22**, 1646-1651.
155. L. M. Rodriguez-Albelo, E. Lopez-Maya, S. Hamad, A. R. Ruiz-Salvador, S. Calero and J. A. Navarro, *Nat Commun*, 2017, **8**, 14457.
156. K. Wang, C. Li, Y. Liang, T. Han, H. Huang, Q. Yang, D. Liu and C. Zhong, *Chemical Engineering Journal*, 2016, **289**, 486-493.
157. F. Vermoortele, B. Bueken, G. Le Bars, B. Van de Voorde, M. Vandichel, K. Houthoofd, A. Vimont, M. Daturi, M. Waroquier, V. Van Speybroeck, C. Kirschhock and D. E. De Vos, *J Am Chem Soc*, 2013, **135**, 11465-11468.
158. N. Al-Janabi, X. Fan and F. R. Siperstein, *J Phys Chem Lett*, 2016, **7**, 1490-1494.
159. S. J. Lee, C. Doussot, A. Baux, L. Liu, G. B. Jameson, C. Richardson, J. J. Pak, F. Trousselet, F.-X. Coudert and S. G. Telfer, *Chemistry of Materials*, 2016, **28**, 368-375.
160. M. H. Sun, S. Z. Huang, L. H. Chen, Y. Li, X. Y. Yang, Z. Y. Yuan and B. L. Su, *Chem Soc Rev*, 2016, **45**, 3479-3563.
161. S. Yuan, L. Zou, J. S. Qin, J. Li, L. Huang, L. Feng, X. Wang, M. Bosch, A. Alsalme, T. Cagin and H. C. Zhou, *Nat Commun*, 2017, **8**, 15356.
162. I. Goettker-Schnetmann, D. M. Heinekey and M. Brookhart, *J. Am. Chem. Soc.*, 2006, **128**, 17114-17119.
163. D. Bradshaw, S. El-Hankari and L. Lupica-Spagnolo, *Chem Soc Rev*, 2014, **43**, 5431-5443.
164. L. G. Qiu, T. Xu, Z. Q. Li, W. Wang, Y. Wu, X. Jiang, X. Y. Tian and L. D. Zhang, *Angew Chem Int Ed Engl*, 2008, **47**, 9487-9491.
165. L. B. Sun, J. R. Li, J. Park and H. C. Zhou, *J Am Chem Soc*, 2012, **134**, 126-129.
166. X.-D. Do, V.-T. Hoang and S. Kaliaguine, *Microporous and Mesoporous Materials*, 2011, **141**, 135-139.
167. G. Cai and H.-L. Jiang, *Angew Chem Int Ed Engl*, 2017, **56**, 563 –567.
168. B. Liu, Y. Li, S. C. Oh, Y. Fang and H. Xi, *RSC Adv.*, 2016, **6**, 61006-61012.
169. J. Park, Z. U. Wang, L. B. Sun, Y. P. Chen and H. C. Zhou, *J Am Chem Soc*, 2012, **134**, 20110-20116.
170. Z. Fang, J. P. Durholt, M. Kauer, W. Zhang, C. Lochenie, B. Jee, B. Albada, N. Metzler-Nolte, A. Poppl, B. Weber, M. Muhler, Y. Wang, R. Schmid and R. A. Fischer, *J Am Chem Soc*, 2014, **136**, 9627-9636.
171. D. Wu, W. Yan, H. Xu, E. Zhang and Q. Li, *Inorganica Chimica Acta*, 2017, **460**, 93-98.
172. W. Zhang, M. Kauer, P. Guo, S. Kunze, S. Cwik, M. Muhler, Y. Wang, K. Epp, G. Kieslich and R. A. Fischer, *European Journal of Inorganic Chemistry*, 2017, **2017**, 925-931.

173. O. Karagiaridi, N. A. Vermeulen, R. C. Klet, T. C. Wang, P. Z. Moghadam, S. S. Al-Juaid, J. F. Stoddart, J. T. Hupp and O. K. Farha, *Inorg Chem*, 2015, **54**, 1785-1790.
174. S. Yuan, W. Lu, Y. P. Chen, Q. Zhang, T. F. Liu, D. Feng, X. Wang, J. Qin and H. C. Zhou, *J Am Chem Soc*, 2015, **137**, 3177-3180.
175. M. Kim, J. F. Cahill, Y. Su, K. A. Prather and S. M. Cohen, *Chem. Sci.*, 2012, **3**, 126-130.
176. Z. Yin, Y. L. Zhou, M. H. Zeng and M. Kurmoo, *Dalton Trans*, 2015, **44**, 5258-5275.
177. S.-H. Lo, C.-H. Chien, Y.-L. Lai, C.-C. Yang, J. J. Lee, D. S. Raja and C.-H. Lin, *J. Mater. Chem. A*, 2013, **1**, 324-329.
178. Y. Yue, A. J. Binder, R. Song, Y. Cui, J. Chen, D. K. Hensley and S. Dai, *Dalton Trans*, 2014, **43**, 17893-17898.
179. Y. Yue, P. F. Fulvio and S. Dai, *Acc Chem Res*, 2015, **48**, 3044-3052.
180. O. V. Gutov, M. Gonzalez Hevia, E. C. Escudero-Adan and A. Shafir, *Inorg Chem*, 2015, **54**, 8396-8400.
181. J. B. DeCoste, T. J. Demasky, M. J. Katz, O. K. Farha and J. T. Hupp, *New J. Chem.*, 2015, **39**, 2396-2399.
182. P. Cheng and Y. H. Hu, *International Journal of Energy Research*, 2016, **40**, 846-852.
183. X.-X. Huang, L.-G. Qiu, W. Zhang, Y.-P. Yuan, X. Jiang, A.-J. Xie, Y.-H. Shen and J.-F. Zhu, *CrystEngComm*, 2012, **14**, 1613-1617.
184. J. M. Taylor, S. Dekura, R. Ikeda and H. Kitagawa, *Chemistry of Materials*, 2015, **27**, 2286-2289.
185. L. Chen, Q. Chen, M. Wu, F. Jiang and M. Hong, *Acc Chem Res*, 2015, **48**, 201-210.
186. T. H. Park, A. J. Hickman, K. Koh, S. Martin, A. G. Wong-Foy, M. S. Sanford and A. J. Matzger, *J Am Chem Soc*, 2011, **133**, 20138-20141.
187. W. Gao, Z. D. Hood and M. Chi, *Acc Chem Res*, 2017, **50**, 787-795.
188. J. Li, S. Cheng, Q. Zhao, P. Long and J. Dong, *International Journal of Hydrogen Energy*, 2009, **34**, 1377-1382.
189. K. Sumida, D. L. Rogow, J. A. Mason, T. M. McDonald, E. D. Bloch, Z. R. Herm, T. H. Bae and J. R. Long, *Chem Rev*, 2012, **112**, 724-781.
190. R. B. Getman, Y. S. Bae, C. E. Wilmer and R. Q. Snurr, *Chem Rev*, 2012, **112**, 703-723.
191. L. Zhu, X. Q. Liu, H. L. Jiang and L. B. Sun, *Chem Rev*, 2017, **117**, 8129-8176.
192. L. E. Kreno, K. Leong, O. K. Farha, M. Allendorf, R. P. Van Duyne and J. T. Hupp, *Chem Rev*, 2012, **112**, 1105-1125.
193. Y. Cui, B. Li, H. He, W. Zhou, B. Chen and G. Qian, *Acc Chem Res*, 2016, **49**, 483-493.
194. P. Horcajada, R. Gref, T. Baati, P. K. Allan, G. Maurin, P. Couvreur, G. Ferey, R. E. Morris and C. Serre, *Chem Rev*, 2012, **112**, 1232-1268.
195. Q. L. Zhu and Q. Xu, *Chem Soc Rev*, 2014, **43**, 5468-5512.
196. T. Kitao, Y. Zhang, S. Kitagawa, B. Wang and T. Uemura, *Chem Soc Rev*, 2017, **46**, 3108-3133.
197. M. L. Foo, R. Matsuda and S. Kitagawa, *Chemistry of Materials*, 2014, **26**, 310-322.
198. M. Zhao, K. Deng, L. He, Y. Liu, G. Li, H. Zhao and Z. Tang, *J Am Chem Soc*, 2014, **136**, 1738-1741.
199. L. Yang, B. Tang and P. Wu, *J. Mater. Chem. A*, 2015, **3**, 15838-15842.
200. X. Yan, X. Hua and S. Komarnenib, *RSC Adv.*, 2014, **4**, 57501–57504.
201. C. Petit and T. J. Bandosz, *Journal of Colloid and Interface Science*, 2015, **447**, 139–151.
202. X. Lian, Y. Fang, E. Joseph, Q. Wang, J. Li, S. Banerjee, C. Lollar, X. Wang and H. C. Zhou, *Chem Soc Rev*, 2017, **46**, 3386-3401.
203. S. Li and F. Huo, *Nanoscale*, 2015, **7**, 7482-7501.
204. J. Gorka, P. F. Fulvio, S. Pikus and M. Jaroniec, *Chem Commun (Camb)*, 2010, **46**, 6798-6800.
205. Study was performed using a Comprehensive Keyword Search using Web of Science search engine
206. Z. Zhang, H. T. Nguyen, S. A. Miller and S. M. Cohen, *Angew Chem Int Ed Engl*, 2015, **54**, 6152-6157.
207. Y. Lin, Hao Lin, H. Wang, Y. Suo, Baihai Li, C. Kong and L. Chen, *J. Mater. Chem. A,*, 2014, **2**, 14658–14665.
208. M. L. Pinto, S. Dias and J. Pires, *ACS Appl Mater Interfaces*, 2013, **5**, 2360−2363.
209. L. Wang, W. Wang, X. Zheng, Z. Li and Z. Xie, *Chem. Eur. J.*, 2017, **23**, 1379-1385.
210. L. Wang, X. Feng, L. Ren, Q. Piao, J. Zhong, Y. Wang, H. Li, Y. Chen and B. Wang, *J Am Chem Soc*, 2015, **137**, 4920-4923.
211. M. J. MacLeod and J. A. Johnson, *Polym. Chem.*, 2017, **8**, 4488-4493.
212. S. Ayala, Z. Zhang and S. M. Cohen, *Chem Commun (Camb)*, 2017, **53**, 3058-3061.

213. C. A. Allen, J. A. Boissonnault, J. Cirera, R. Gulland, F. Paesani and S. M. Cohen, *Chem Commun (Camb)*, 2013, **49**, 3200-3202.
214. Z. Zhang, H. T. Nguyen, S. A. Miller, A. M. Ploskonka, J. B. DeCoste and S. M. Cohen, *J Am Chem Soc*, 2016, **138**, 920-925.
215. W. Li, Q. Meng, C. Zhang and G. Zhang, *Chem. Eur. J.*, 2015, **21**, 7224-7230.
216. G. Chen, W. J. Koros and C. W. Jones, *ACS Appl. Mater. Interfaces* 2016, **8**, 9700–9709.
217. H. B. Luo, M. Wang, S. X. Liu, C. Xue, Z. F. Tian, Y. Zou and X. M. Ren, *Inorg Chem*, 2017, **56**, 4169-4175.
218. N. Angulakshmi, R. S. Kumar, M. A. Kulandainathan and A. M. Stephan, *The Journal of Physical Chemistry C*, 2014, **118**, 24240-24247.
219. K. Sumida, K. Liang, J. Reboul, I. A. Ibarra, S. Furukawa and P. Falcaro, *Chemistry of Materials*, 2017, **29**, 2626-2645.
220. K. M. L. Taylor, William J. Rieter and W. Lin, *J Am Chem Soc*, 2008, **130**, 14358–14359.
221. P. Falcaro, R. Ricco, A. Yazdi, I. Imaz, S. Furukawa, D. Maspoch, R. Ameloot, J. D. Evans and C. J. Doonan, *Coordination Chemistry Reviews*, 2016, **307**, 237-254.
222. A. Dhakshinamoorthy and H. Garcia, *Chem Soc Rev*, 2012, **41**, 5262-5284.
223. K. Ariga, Q. Ji, J. P. Hill, Y. Bando and M. Aono, *NPG Asia Materials*, 2012, **4**.
224. G. Lu, S. Li, Z. Guo, O. K. Farha, B. G. Hauser, X. Qi, Y. Wang, X. Wang, S. Han, X. Liu, J. S. DuChene, H. Zhang, Q. Zhang, X. Chen, J. Ma, S. C. Loo, W. D. Wei, Y. Yang, J. T. Hupp and F. Huo, *Nat Chem*, 2012, **4**, 310-316.
225. R. L. Martin and M. Haranczyk, *Crystal Growth & Design*, 2013, **13**, 4208-4212.
226. M. Meilikhov, K. Yusenko, D. Esken, S. Turner, G. Van Tendeloo and R. A. Fischer, *European Journal of Inorganic Chemistry*, 2010, **2010**, 3701-3714.
227. Z. Ulker, I. Erucar, S. Keskin and C. Erkey, *Microporous and Mesoporous Materials*, 2013, **170**, 352-358.
228. J. Aguilera-Sigalat and D. Bradshaw, *Coordination Chemistry Reviews*, 2016, **307**, 267-291.
229. J. Juan-Alcañiz, J. Gascon and F. Kapteijn, *Journal of Materials Chemistry*, 2012, **22**.
230. B. R. Cuenya, *Thin Solid Films*, 2010, **518**, 3127-3150.
231. Q. L. Zhu, J. Li and Q. Xu, *J Am Chem Soc*, 2013, **135**, 10210-10213.
232. K. Na, K. M. Choi, O. M. Yaghi and G. A. Somorjai, *Nano Lett*, 2014, **14**, 5979-5983.
233. K. M. Choi, K. Na, G. A. Somorjai and O. M. Yaghi, *J Am Chem Soc*, 2015, **137**, 7810-7816.
234. A. Henschel, K. Gedrich, R. Kraehnert and S. Kaskel, *Chem Commun (Camb)*, 2008, DOI: 10.1039/b718371b, 4192-4194.
235. W. Du, G. Chen, R. Nie, Y. Li and Z. Hou, *Catalysis Communications*, 2013, **41**, 56-59.
236. A. Aijaz, A. Karkamkar, Y. J. Choi, N. Tsumori, E. Ronnebro, T. Autrey, H. Shioyama and Q. Xu, *J Am Chem Soc*, 2012, **134**, 13926-13929.
237. M. Zhao, K. Yuan, Y. Wang, G. Li, J. Guo, L. Gu, W. Hu, H. Zhao and Z. Tang, *Nature*, 2016, **539**, 76-80.
238. L. Zhang, Z. Su, F. Jiang, Y. Zhou, W. Xu and M. Hong, *Tetrahedron*, 2013, **69**, 9237-9244.
239. B. Yuan, Y. Pan, Y. Li, B. Yin and H. Jiang, *Angew Chem Int Ed Engl*, 2010, **49**, 4054-4058.
240. S. Gao, N. Zhao, M. Shu and S. Che, *Applied Catalysis A: General*, 2010, **388**, 196-201.
241. V. Pascanu, Q. Yao, A. Bermejo Gomez, M. Gustafsson, Y. Yun, W. Wan, L. Samain, X. Zou and B. Martin-Matute, *Chemistry*, 2013, **19**, 17483-17493.
242. A. K. Gupta, D. De, R. Katoch, A. Garg and P. K. Bharadwaj, *Inorg Chem*, 2017, **56**, 4698-4706.
243. Y.-Z. Chen, Z. U. Wang, H. Wang, u. Lu, S.-H. Yu and H.-L. Jiang, *J Am Chem Soc*, 2017, **139**, 2035-2044.
244. Y. Wanga, Y. Zhanga, Z. Jiangb, G. Jianga, Z. Zhaoa, Q. Wua, Y. Liua, Q. Xua, A. Duana and C. Xu, *Applied Catalysis B: Environmental*, 2016, 307-314.
245. C. Wang, K. E. deKrafft and W. Lin, *J Am Chem Soc*, 2012, **134**, 7211-7214.
246. C. Zlotea, R. Campesi, F. Cuevas, E. Leroy, P. Dibandjo, C. Volkringer, h. Loiseau, G. Férey and M. Latroche, *J Am Chem Soc*, 2010, **132**, 2991-2997.
247. D. Banerjee, A. J. Cairns, J. Liu, R. K. Motkuri, S. K. Nune, C. A. Fernandez, R. Krishna, D. M. Strachan and P. K. Thallapally, *Acc Chem Res*, 2015, **48**, 211-219.
248. Y. Hu, J. Liao, D. Wang and G. Li, *Anal Chem*, 2014, **86**, 3955-3963.
249. K. Sugikawa, Y. Furukawa and K. Sada, *Chemistry of Materials*, 2011, **23**, 3132-3134.

250. M. Saikia, D. Bhuyan and L. Saikia, *New J. Chem.*, 2015, **39**, 64-67.
251. S. H. Huo and X. P. Yan, *Analyst*, 2012, **137**, 3445-3451.
252. F. Ke, L.-G. Qiu, Y.-P. Yuan, X. Jiang and J.-F. Zhu, *Journal of Materials Chemistry*, 2012, **22**.
253. Z. Jiang and Y. Li, *Journal of the Taiwan Institute of Chemical Engineers*, 2016, 373-379.
254. T. Khezeli and A. Daneshfar, *RSC Adv.*, 2015, **5**, 65264-65273.
255. J. M. Zamaro, N. C. Pérez, E. E. Miró, C. Casado, B. Seoane, C. Téllez and J. Coronas, *Chemical Engineering Journal*, 2012, **195-196**, 180-187.
256. Y. Chen, D. Lv, J. Wu, J. Xiao, H. Xi, Q. Xia and Z. Li, *Chemical Engineering Journal*, **308**, 1065-1072.
257. H. Zhou, J. Zhang, J. Zhang, X.-F. Yan, X.-P. Shen and A.-H. Yuan, *Inorganic Chemistry Communications*, 2015, **54**, 54-56.
258. B. Levasseur, C. Petit and T. J. Bandosz, *Applied Materials and Interfaces*, 2010, **12**, 3606-3613.
259. X. Zhou, W. Huang, J. Shi, Z. Zhao, Q. Xia, i. Li, H. Wanga and Z. Li, *journal of Materials Chemistry A*, 2014, 4722-4730.
260. X. Suna, Q. XiabN, Z. Zhaoa, Y. Lia and Z. Li, *Chemical Engineering Journal*, 2014, **239**, 226-232.
261. C. Yang, S. Wu, J. Cheng and Y. Chen, *Journal of Alloys and Compounds*, 2016, **687**, 804-812.
262. L. Li, X. L. Liu, H. Y. Geng, B. Hu, G. W. Song and Z. S. Xu, *Journal of materials Chemistry A*, 2013, 10292-10299.
263. W. Bao, Z. Zhang, Y. Qu, C. Zhou, X. Wang and J. Li, *Journal of Alloys and Compounds*, 2014, **582**, 334-340.
264. I. Ahmed, N. A. Khan and S. H. Jhung, *Inorg Chem*, 2013, **52**, 14155-14161.
265. M. Anbia and V. Hoseini, *Chemical Engineering Journal*, 2012, **191**, 326-330.
266. K. P. Prasanth, P. Rallapalli, M. C. Raj, H. C. Bajaj and R. V. Jasra, *International Journal of Hydrogen Energy*, 2011, **36**, 7594-7601.
267. Z. Xiang, Z. Hu, D. Cao, W. Yang, J. Lu, B. Han and W. Wang, *Angew Chem Int Ed Engl*, 2011, **50**, 491-494.
268. T. Han, Y. Xiao, M. Tong, H. Huang, D. Liu, L. Wang and C. Zhong, *Chemical Engineering Journal*, 2015, **275**, 134-141.
269. M. Jahan, Q. Bao and K. P. Loh, *J Am Chem Soc*, 2012, **134**, 6707-6713.
270. P. B. Somayajulu Rallapalli, M. C. Raj, D. V. Patil, K. P. Prasanth, R. S. Somani and H. C. Bajaj, *International Journal of Energy Research*, 2013, **37**, 746-753.
271. F. N. Azad, M. Ghaedi, K. Dashtian, S. Hajati and V. Pezeshkpour, *Ultrason Sonochem*, 2016, **31**, 383-393.
272. H. Wang, X. Yuana, Y. Wud, G. Zeng, X. Chen, L. Leng and H. Li, *Applied Catalysis B: Enviormental*, 2015, **174-175**, 445-454.
273. Y. Han, P. Qi, X. Feng, S. Li, X. Fu, H. Li, Y. Chen, J. Zhou, X. Li and B. Wang, *ACS Appl Mater Interfaces*, 2015, **7**, 2178-2182.
274. A. Ahmed, M. Forster, R. Clowes, D. Bradshaw, P. Myers and H. Zhang, *Journal of Materials Chemistry A*, 2013, **1**.
275. W. Ying, Y. Mao, X. Wang, Y. Guo, H. He, Z. Ye, S. T. Lee and X. Peng, *ChemSusChem*, 2017, **10**, 1346-1350.
276. X. Lin, G. Gao, L. Zheng, Y. Chi and G. Chen, *Anal Chem*, 2014, **86**, 1223-1228.
277. A. R. Chowdhuri, T. Singh, S. K. Ghosh and S. K. Sahu, *ACS Appl Mater Interfaces*, 2016, **8**, 16573-16583.
278. W. Salomon, C. Roch-Marchal, P. Mialane, P. Rouschmeyer, C. Serre, M. Haouas, F. Taulelle, S. Yang, L. Ruhlmann and A. Dolbecq, *Chem Commun (Camb)*, 2015, **51**, 2972-2975.
279. F. Zhang, Y. Jin, J. Shi, Y. Zhong, W. Zhu and M. S. El-Shall, *Chemical Engineering Journal*, 2015, **269**, 236-244.
280. C. M. Granadeiro, A. D. S. Barbosa, P. Silva, F. A. A. Paz, V. K. Saini, J. Pires, B. de Castro, S. S. Balula and L. Cunha-Silva, *Applied Catalysis A: General*, 2013, **453**, 316-326.
281. C. M. Granadeiro, P. Silva, V. K. Saini, F. A. A. Paz, J. Pires, L. Cunha-Silva and S. S. Balula, *Catalysis Today*, 2013, **218-219**, 35-42.
282. R. A. Sheldon and S. van Pelt, *Chem Soc Rev*, 2013, **42**, 6223-6235.
283. M. B. Majewski, A. J. Howarth, P. Li, M. R. Wasielewski, J. T. Hupp and O. K. Farha, *CrystEngComm*, 2017, **19**, 4082-4091.
284. S. Patra, T. Hidalgo Crespo, A. Permyakova, C. Sicard, C. Serre, A. Chaussé, N. Steunou and L. Legrand, *J. Mater. Chem. B*, 2015, **3**, 8983-8992.
285. F.-X. Qin, S.-Y. Jia, F.-F. Wang, S.-H. Wu, J. Song and Y. Liu, *Catalysis Science & Technology*, 2013, **3**.

286. S.-L. Cao, D.-M. Yue, X.-H. Li, T. J. Smith, N. Li, M.-H. Zong, H. Wu, Y.-Z. Ma‖ and W.-Y. Lou, *ACS Sustainable Chem. Eng.*, 2016, **4**, 3586-3595.
287. S. Jung, Y. Kim, S. J. Kim, T. H. Kwon, S. Huh and S. Park, *Chem Commun (Camb)*, 2011, **47**, 2904-2906.
288. K. Liang, R. Ricco, C. M. Doherty, M. J. Styles, S. Bell, N. Kirby, S. Mudie, D. Haylock, A. J. Hill, C. J. Doonan and P. Falcaro, *Nat Commun*, 2015, **6**, 7240.
289. F. Lyu, Y. Zhang, R. N. Zare, J. Ge and Z. Liu, *Nano Lett*, 2014, **14**, 5761-5765.
290. J. H. Harding, *Chemical Reviews*, 2008, **108**, 4823–4854.
291. V. Lykourinou, Y. Chen, X. S. Wang, L. Meng, T. Hoang, L. J. Ming, R. L. Musselman and S. Ma, *J Am Chem Soc*, 2011, **133**, 10382-10385.
292. D. Feng, T. F. Liu, J. Su, M. Bosch, Z. Wei, W. Wan, D. Yuan, Y. P. Chen, X. Wang, K. Wang, X. Lian, Z. Y. Gu, J. Park, X. Zou and H. C. Zhou, *Nat Commun*, 2015, **6**, 5979.
293. X. Lian, Y. P. Chen, T. F. Liu and H. C. Zhou, *Chem Sci*, 2016, **7**, 6969-6973.
294. P. Li, Justin A. Modica, Ashlee J. Howarth, E. Vargas L, Peyman Z. Moghadam, Randall Q. Snurr, M. Mrksich, Joseph T. Hupp and Omar K. Farha, *Chem*, 2016, **1**, 154-169.

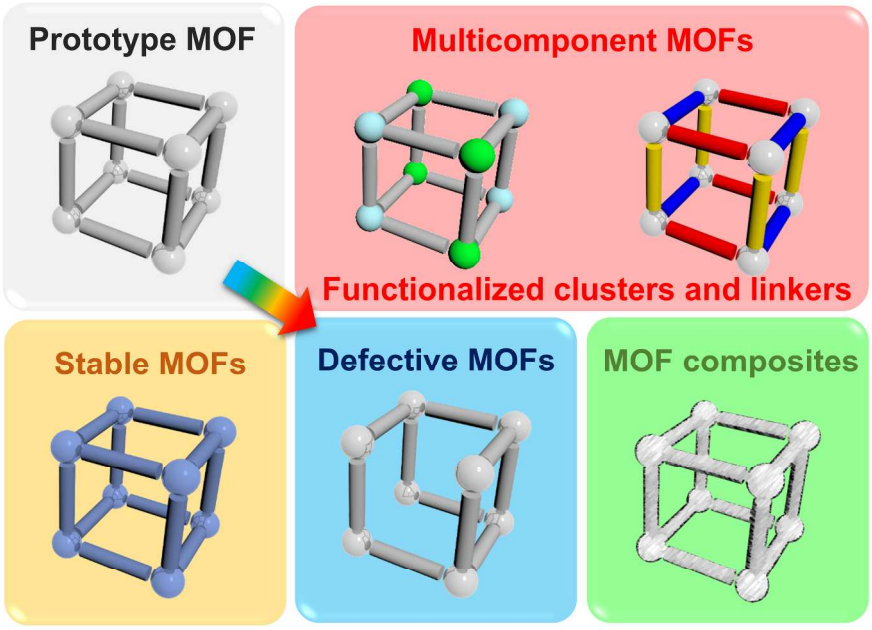

127x90mm (600 x 600 DPI)